

complexes in tetragonally distorted octahedral, square-base-pyramidal, or square-planar stereochemistries, all copper(II) geometries associated with a $d_{x^2-y^2}$ ground state. The $A_{||}$ values are higher than those found in the copper bis(amino acidato) complexes that contain the CuN_2O_2 chromophore,^{13,35} suggesting that a greater extent of the tetragonal elongation of the potential apical coordination sites is probably present in the copper(II) dipeptide systems. Furthermore, the EPR parameters show the same values found for $\text{Cu}(\text{H}_2\text{L})$ species of Leu-Ileu diastereoisomers,¹ suggesting that the sulfur atoms are not involved in the coordination. On the other hand the small difference in $A_{||}$ values, giving evidence of stereoselectivity, cannot be attributed to a different interaction of the metal ion with the solvent or to its different geometries in the complexes of two diastereoisomers. The $A_{||}$ data parallel those found in the case of the EPR study of the polycrystalline material obtained by doping $\text{Zn}(\text{L-Met})_2$,³⁶ which is isomorphous with the analogous copper bis complex. The molecular structure showed a trans arrangement of the two amino acidate molecules chelated to the copper atom. The coordination around the copper(II) atom is essentially square planar even if interactions with neighboring methionine oxygen atoms (2.751 or 2.676 Å) coming from carboxylate groups are important to build up the crystal packing. The $A_{||}$ value of $182.5 \times 10^{-3} \text{ cm}^{-1}$ was obtained in situation like that in the copper(II) complex with the L,D-isomer. Thus, to explain the higher $A_{||}$ value for the L,L-dipeptide complex than for the corresponding D,L-isomer species, other factors must be invoked. In the $\text{Cu}(\text{H}_2\text{L})$ with L,L-diastereoisomeric molecules the side chains can interact above the coordination plane; as a consequence of this solvophobic inter-

action, some "stiffening" may be experienced by the basal plane. This interaction could constrain the donor atoms of the dipeptide coordinated to the metal ion to achieve a quasi-ideal planar conformation. On the contrary, when this interaction is not possible (as for the D,L-dipeptide complex), the lower $A_{||}$ value may be due to the presence of a small tetrahedral distortion.

This suggestion seems to be justified because it is well-known from Freeman's crystallographic work³⁷ that the basal plane formed by the dipeptide chelate group is distorted toward a tetrahedral situation. Thus, the thermodynamic stereoselectivity in copper(II) complex formation with the methionylmethionine peptide is due to the solvophobic forces and not to the bonding of sulfur atoms. If the thioetheral atoms were involved in the coordination to copper(II), the metal ion would have shown a different coordination number and geometry in the two diastereoisomeric complexes. The $A_{||}$ values exclude this hypothesis.

As previously reported^{1,14} the thermodynamic stereoselectivity is more evident on the basis of the enthalpy changes with respect to the free energy ones. The ΔH° value of the $\text{Cu}(\text{Met-Met})$ complex is nearly equal to the ΔH° of $\text{Cu}(\text{L-Leu-L-Ileu})$, showing that the elongation of the side chain does not involve an enhancement of the solvophobic interaction, such as recently noted by other authors.³⁸

Acknowledgment. We thank the MPI (Italy) for partial support.

Registry No. $\text{Cu}(\text{D-Met-L-Met})$, 109218-19-1; $\text{Cu}(\text{Met-Met})$, 109281-40-5; L-methionyl-L-methionine, 7349-78-2; D-methionyl-L-methionine, 89680-17-1.

(35) Szabo-Planke, T.; Horváth, L. *J. Acta Chim. Hung.* **1983**, *114*, 15.

(36) Ou, C.; Powers, D. A.; Thich, J. A.; Felthouse, T. R.; Hendrickson, D. N.; Potenza, J. A.; Schugar, H. J. *Inorg. Chem.* **1978**, *17*, 34.

(37) Freeman, H. C. *The Biochemistry of Copper*; Peisach, J., Aisen, P., Blumberg, W. E., Eds.; Academic: New York, 1966; p 77.

(38) Liang, G.; Tribollet, R.; Sigel, H. *Proceedings of the XXIV International Conference on Coordination Chemistry*; Athens, Greece, 1986; p 199.

Contribution from the Department of Chemistry,
University of Pittsburgh, Pittsburgh, Pennsylvania 15260

Pentacyanoferrate(II/III) Complexes of 2-Substituted Imidazoles and Imidazoles ($\text{R} = \text{CH}_3, \text{CHO}, \text{CO}_2^-$)

Erin M. Sabo, Rex E. Shepherd,* Melinda S. Rau, and Michael G. Elliott

Received March 17, 1987

$(\text{CN})_5\text{Fe}^{\text{III}}\text{L}^{2-}$ and $(\text{CN})_5\text{Fe}^{\text{III}}\text{L}^{3-}$ complexes have been studied with 2-substituted imidazoles (RimH ; $\text{R} = \text{CH}_3, \text{CHO}, \text{CO}_2^-$). $2\text{CO}_2\text{imH}^-$ exhibits no complexation of $(\text{CN})_5\text{Fe}^{3+}$, as shown by ^{13}C NMR with up to 10-fold excess ligand, but forms the Fe(III) derivative $(\text{CN})_5\text{Fe}(2\text{CO}_2\text{imH})^{3-}$. The formation constant of this species, $K_f \approx 35 \text{ M}^{-1}$, is reduced by 9.7×10^3 relative to that for imH . The Fe(III) complexes exhibit LMCT transitions with the characteristic imidazole $d\pi \leftarrow (\pi_1)_L$ bands at 450, 460, 475, and 505 nm with $\text{R} = \text{CHO}, \text{CO}_2^-, \text{H}$, and CH_3 , respectively, in concert with the σ_p substituent constants. Imidazoles are generally poor π acceptors, but 2CHOimH acts as a strong π -acceptor ligand toward $(\text{CN})_5\text{Fe}^{3+}$; $(\text{CN})_5\text{Fe}^{\text{II}}(2\text{CHOimH})^{3-}$ exhibits an MLCT transition at 454 nm, similar to that for the pyrazine complex. The standard reduction potential for the $(\text{CN})_5\text{Fe}(2\text{CHOimH})^{2-/3-}$ complex is 0.42 V, ca. 0.06 V more favorable than $(\text{CN})_5\text{Fe}(\text{imH})^{2-/3-}$. The imidazolato forms of the Fe(III) complexes exhibit characteristic $d\pi \leftarrow (\pi_{2,n})_L$ transitions at 428, 438, and 448 nm for $\text{R} = \text{CHO}, \text{H}$, and CH_3 , respectively, increasing in the order of the substituent's releasing influence. The imidazolates undergo solvent-assisted dissociation to form $(\text{CN})_5\text{FeOH}^{3-}$ and the free ligand. The rate constant for dissociation of the $2\text{CH}_3\text{im}^-$ derivative is $k_d = (2.33 \pm 0.08) \times 10^{-3} \text{ s}^{-1}$, determined at 25.0 °C, 0.50 M OH^- , and $\mu = 1.00$ (NaCl), and $(1.9 \pm 0.3) \times 10^{-3} \text{ s}^{-1}$, at 0.10 M OH^- and $\mu = 1.00$. The steric enhancement for dissociation of $2\text{CH}_3\text{im}^-$ vs. im^- is a factor of ca. 8.9. The dissociation is prone to catalysis by traces of the Fe(II) complex. The catalysis may be blocked by the presence of excess $\text{S}_2\text{O}_8^{2-}$, but competitive ligand oxidation generates a mixture of $(\text{CN})_5\text{Fe}^{\text{III}}(2\text{CH}_3\text{imH})^{2-}$ and $(\text{CN})_5\text{Fe}^{\text{III}}(2\text{CO}_2\text{imH})^{3-}$. Dissociation of the imidazolato form of the latter is more rapid. The lability of $(\text{CN})_5\text{Fe}^{\text{III}}(2\text{CO}_2\text{imH})^{3-}$ was studied by using (dimethylamino)pyridine (dmapy) as a scavenger for $(\text{CN})_5\text{FeOH}^{2-}$. dmapy substitutes on $(\text{CN})_5\text{FeOH}^{2-}$ and the $\text{Fe}_2(\text{CN})_{10}^{4-}$ dimer with rate constants of $12.2 \text{ M}^{-1} \text{ s}^{-1}$ and $2.0 \times 10^{-3} \text{ s}^{-1}$, respectively. $(\text{CN})_5\text{Fe}^{\text{III}}(2\text{CO}_2\text{imH})^{3-}$ dissociates at least a power of 10 more slowly than the substitution of dmapy on $\text{Fe}_2(\text{CN})_{10}^{4-}$. Both the free ligand $2\text{CO}_2\text{imH}^-$ and its Fe(III) complex $(\text{CN})_5\text{Fe}(2\text{CO}_2\text{imH})^{3-}$ react with H_2O_2 (but not $\text{S}_2\text{O}_8^{2-}$) within 24 h to form a new imidazole ligand and a $(\text{CN})_5\text{Fe}(\text{RimH})^{2-}$ complex. However, the imidazole products of the two processes are different, leading to what appears to be $\text{R} = \text{OH}$ for the free ligand and $\text{R} = \text{CH}_2(\text{OH})$ for the coordinated ligand.

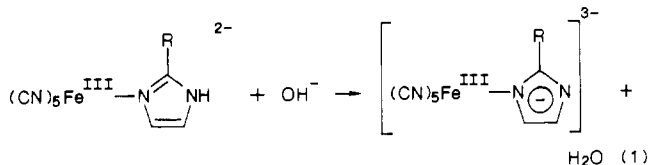
Introduction

Dissociation of metal ion-imidazolato bonds may be important in the function of certain enzymes such as superoxide dismutase. Deprotonation of imidazole coordinated to $(\text{CN})_5\text{Fe}^{2+}$ and dissociation of the imidazolato, Rim^- , ligand has been studied previously by Johnson et al.¹ with $\text{R} = \text{H}$. The reaction proceeds

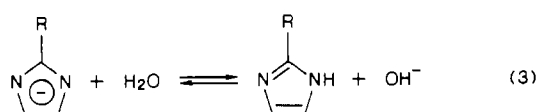
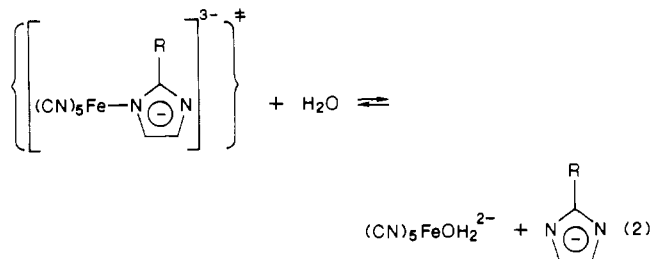
by a dissociative pathway in which the Fe(III)-imidazolato bond is very much stretched and weakened in the transition state (\ddagger).¹ Rim^- is subsequently replaced by OH^- by two possible routes. One

(1) Johnson, C. R.; Shepherd, R. E.; Marr, B.; O'Donnell, S.; Dressick, W. *J. Am. Chem. Soc.* **1980**, *102*, 6227-6235.

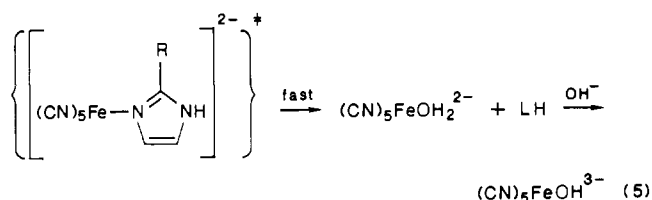
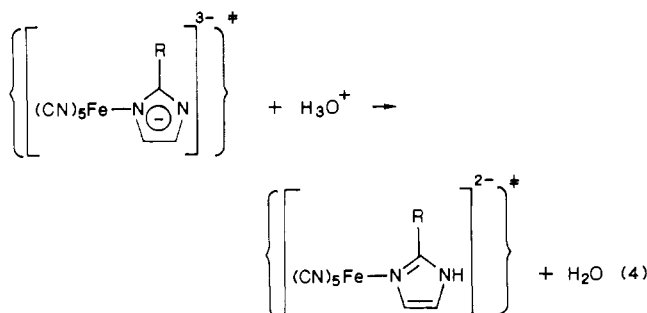
is with solvent-assisted displacement and one is with H_3O^+ assistance, making LH a good leaving group (eq 4). The con-



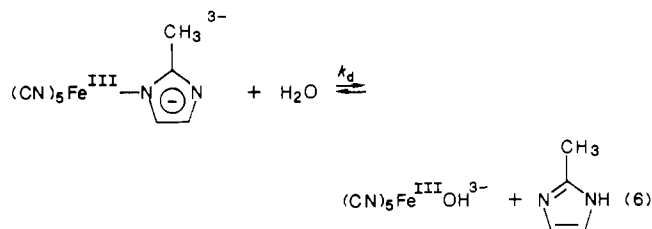
path 1



path 2



centration of the free imidazolato ligand will be very small due to equilibrium 3. This favors the dissociation of Rim^- by Le Chatelier's law at high pH. In this current work the system with $\text{R} = \text{CH}_3$ was studied in order to determine the effect of steric hindrance on the rate of the overall reaction for dissociation of the imidazolato (eq 6).



A side reaction prompted the study of complexes of the $\text{R} = \text{CO}_2^-$ and $\text{R} = \text{CHO}$ ligands toward $(\text{CN})_5\text{Fe}^{2-}$ and $(\text{NH}_3)_5\text{Ru}^{3+}$. The anionic nature of 2-carboxylatoimidazole significantly alters its capacity to coordinate to either $(\text{CN})_5\text{Fe}^{2-}$ or $(\text{CN})_5\text{Fe}^{3-}$ but not to the cationic $(\text{NH}_3)_5\text{Ru}^{2+}$ and $(\text{NH}_3)_5\text{Ru}^{3+}$ centers.¹²

The changing π -acceptor or π -donor character of the substituted imidazole ring is a subject of considerable current interest. Imidazoles and methylated imidazoles show very little π -acceptor character² but are good π donors. The π -donor influence has

shown up in the Mössbauer quadrupole splitting parameters, in the $\text{p}K_a$ of the coordinated imidazole form, and in the electrochemical behavior of imidazole-pentacyanoferrate(III) and imidazole-pentaammineruthenium(III) complexes.²⁻⁴

The LMCT spectral transitions for the same two series of complexes exhibit a strong dependence on the π -donor ability of substituted imidazoles.^{4,5} An exception to the normally low π -acceptor power of most imidazoles was recently reported in the study of the 4-nitroimidazole (4-NIMH) and 4-nitroimidazolato complexes of pentacyanoferrate(II).⁶ Eaton and Watkins showed the 4- NO_2 substituent produces a strong π -acceptor capability for this imidazole; the resultant complexes exhibit the usual MLCT bands and additional stabilization of the lower Fe(II) oxidation state that are characteristic of very good π -acceptor ligands.⁶ 4-NIM can even stabilize the Fe(I) reduction product of $(\text{CN})_5\text{Fe}(4\text{-NIMH})^{3-}$. Various spectral and chemical properties suggest the 4-nitroimidazolato complex is comparable to 4-pyridylpyridinium ion as a good π -acceptor toward $(\text{CN})_5\text{Fe}^{3-}$, but it is a much poorer π donor in the imidazolato form than the parent imidazolato ligand ($\text{R} = \text{H}$) toward $(\text{CN})_5\text{Fe}^{2-}$. These effects are consistent with substituent constants, σ_p , of organic chemistry, which place $-\text{NO}_2$ as one of the most electron withdrawing groups ($\sigma_p = 0.78$).⁷ The 2-substituted imidazoles of this study have revealed additional cases ($\text{R} = \text{CHO}$, CO_2^-) where significant alteration of the π -acceptor and π -donor power of the imidazole ring toward a transition-metal center is detectable. The values of σ_p are given as 0.22 and 0.13 for $\text{R} = \text{CHO}$ and $\text{R} = \text{CO}_2\text{H}$, respectively.⁷ Results in harmony with the anticipated withdrawing power of the groups, intermediate between $\text{R} = \text{H}$ or CH_3 and $\text{R} = \text{NO}_2$, are reported in this work.

Experimental Section

Reagents. $\text{Na}_3[(\text{CN})_5\text{FeNH}_3]\cdot 3\text{H}_2\text{O}$ was prepared from $\text{Na}_2[(\text{CN})_5\text{FeNO}]\cdot 2\text{H}_2\text{O}$ as described previously.⁸ 4,5-Imidazolecarboxylic acid was obtained from ICN Pharmaceuticals. Triethylorthoformate, $\text{K}_2\text{S}_2\text{O}_8$, 2-methylimidazole (2CH₃imH), 2-imidazolecarboxaldehyde (2CHOimH), and 4-(dimethylamino)pyridine (dmapy) were obtained from Aldrich. Sodium chloride was obtained from Mallinckrodt (analytical reagent grade).

Kinetic Studies of the $(\text{CN})_5\text{Fe}(2\text{CH}_3\text{im})^{2-}$ Complex. $\text{Na}_3[(\text{CN})_5\text{FeNH}_3]\cdot 3\text{H}_2\text{O}$ was weighed out as was the appropriate amount of 2-methylimidazole to be in 10–20 times molar excess such that the final $[(\text{CN})_5\text{Fe}(2\text{CH}_3\text{im})^{2-}]$ was 2.817×10^{-2} M after mixing in H_2O . After the ligand was completely dissolved, $\text{Na}_3[(\text{CN})_5\text{FeNH}_3]\cdot 3\text{H}_2\text{O}$ was added while magnetic stirring was maintained with a rice-grain-sized bar. Ten minutes was allowed for complexation. The oxidant, $\text{K}_2\text{S}_2\text{O}_8$, was added as a known excess of the iron complex, and the solution was allowed time to undergo complete oxidation of the Fe^{II} to Fe^{III} . The oxidation is observed as an immediate change in the color of the solution from clear yellow to very dark purplish red.

The appropriate amount of NaCl to make the ionic strength of a 10.00-mL solution of NaOH equal to 1.00 was weighed out and mixed with the desired solution of NaOH. A 9.00-mL aliquot was equilibrated at 25.0 °C for mixing with 1.00 mL of the $[(\text{CN})_5\text{Fe}(2\text{CH}_3\text{im})]^{3-}$ solution, also equilibrated at 25.0 °C. The NaOH/NaCl was added to the $[(\text{CN})_5\text{Fe}^{\text{III}}(2\text{CH}_3\text{im})]^{3-}$ simultaneously with the start of a timer. The solutions were thoroughly mixed by pouring back into each original container several times. The resulting green solution was placed in a 1-cm cell and the decrease in absorbance at 500 nm monitored as a function of time. The instrument used was a Varian Cary 118C spec-

- (2) Johnson, C. R.; Henderson, W. W.; Shepherd, R. E. *Inorg. Chem.* **1984**, *23*, 2754–2763.
- (3) Johnson, C. R.; Shepherd, R. E. *Inorg. Chem.* **1983**, *22*, 3506–3513.
- (4) Johnson, C. R.; Shepherd, R. E. *Synth. React. Inorg. Met.-Org. Chem.* **1984**, *14*, 339–353.
- (5) (a) Hoq, M. F.; Shepherd, R. E. *Inorg. Chem.* **1984**, *23*, 1851–1858. (b) Jones, C. M.; Johnson, C. R.; Asher, S. A.; Shepherd, R. E. *J. Am. Chem. Soc.* **1985**, *107*, 3772–3780.
- (6) Eaton, D. R.; Watkins, J. M. *Inorg. Chem.* **1985**, *24*, 1424–1431.
- (7) Gould, E. S. *Mechanism and Structure in Organic Chemistry*; Holt, Rinehart and Winston: New York, 1959; p 221.
- (8) Ernhoffer, R.; Kovacs, D.; Subak, E.; Shepherd, R. E. *J. Chem. Educ.* **1978**, *55*, 610–611.
- (9) The ^{13}C shifts of the cyanide resonances compare with 177.3 ppm for $\text{Fe}(\text{CN})_6^{4-}$: Figard, J. E.; Paukstelis, J. V.; Byrne, E. F.; Peterson, J. D. *J. Am. Chem. Soc.* **1977**, *99*, 8417–8425.

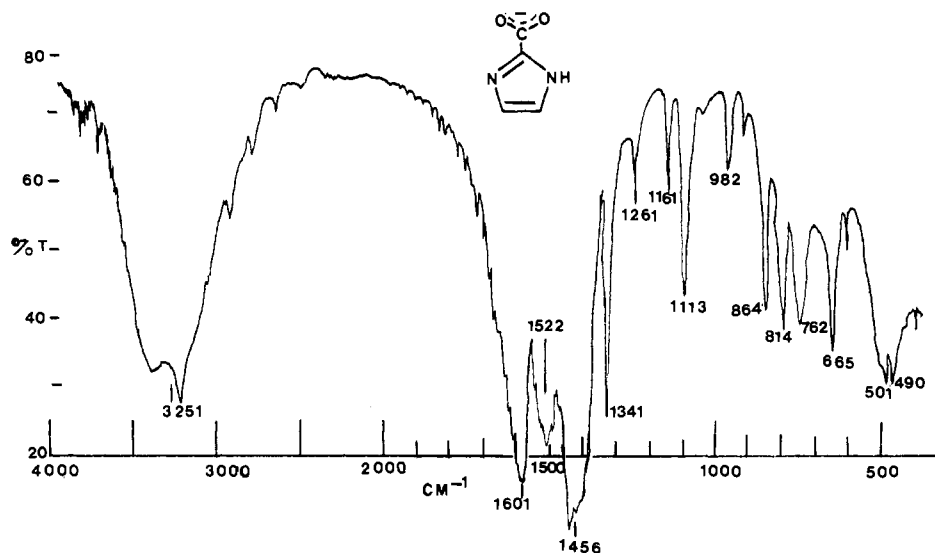


Figure 1. FTIR spectrum of Li(2CO₂imH) in KBr (16 scans, 4-cm⁻¹ resolution).

Table I. LMCT Spectra of Imidazole Complexes (Absorbance Maximum, 10³ cm⁻¹ (λ, nm))

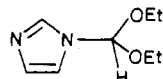
ligand	(CN) ₅ Fe ^{III} ^a			(NH ₃) ₅ Ru ^{III} ^b		
	dπ ← (π ₁) _L	dπ ← (π _{2,n}) _L	dπ ← σ _{CN}	dπ ← (π ₁) _L	dπ ← (π _{2,n}) _L	
imidazole	21.1 (475)	24.8 (403)	28.1 (356)	23.5 (425)	33.7 (297)	39.2 (255)
imidazolate	16.0 (625)	22.8 (438)		16.1 (620)	27.2 (367)	39.2 (255)
2-methylimidazole	19.8 (505)	24.8 (404)	27.9 (358)	21.5 (465)	32.9 (304)	37.0 (270)
2-methylimidazolate		22.5 (448)		16.1 (620)	27.2 (367)	39.2 (255)
2-carboxylatoimidazole	21.7 (460)	24.9 (401)		23.3 (430)		
2-carboxylatoimidazolate		23.0 (435)		18.3 (545)		
2-imidazolecarboxaldehyde	22.2 (450)	24.6 (406)				
2-imidazolotocarboxaldehyde	17.4 (575)	23.4 (428)				
4,5-dicarboxylatoimidazole	19.4 (515)	24.7 (405)				

^aData from ref 2 and this work. ^bData from ref 2 and 12.

trophotometer designed so that water from the temperature bath maintained the cell block at 25.0 °C.

The data were collected as absorbance vs. time; the program VAINF2 was used to estimate A_{∞} and k_{obsd} for each run.¹ This A_{∞} was used to calculate $-\ln(A - A_{\infty})$, and this value was then plotted against time by using the program DIGPLT.¹⁰ This curve should be linear and can be used to evaluate regions of deviation. The slope of this line is the observed rate. Both programs gave values for k_{obsd} that were in agreement, when catalytic problems, which are described in the main text, were absent.

Lithium 2-Imidazolecarboxylate. The protected



precursor compound was prepared by reaction of imidazole with triethyl orthoformate, rigorously following the method of Curtis and Brown.¹¹ After removal of excess orthoformate, the precursor product was fractionally distilled under vacuum to give a product having NMR properties identical with those reported by Curtis and Brown.¹¹ The precursor complex was converted to the lithium salt of 2-imidazolecarboxylic acid in a modification of Curtis and Brown's procedure.¹¹ The precursor was treated with *n*-butyllithium and then mixed with crushed dry ice in dry THF at -40 °C (acetone/dry ice bath). As the 2-imidazolecarboxylic acid is unstable with respect to decarboxylation, the ligand was stored as the salt of 2CO₂imH⁻. The isolated salt Li(2CO₂imH) exhibited the anticipated ν_{CO₂} at 1601 cm⁻¹ (Figure 1). The carboxylic acid form exhibited a singlet for the C-4 and C-5 hydrogens at δ 7.28 in D₂O. It was discovered that the product may be contaminated by imidazole formed as a side reaction to the addition of the lithium carbanion to solid CO₂. The infrared spectrum of the pure product is given in Figure 1.

Spectral Characterization. Ultraviolet-visible spectra were recorded on the same Varian-Cary 118C spectrophotometer as used in the kinetic studies. NMR spectra were obtained with a WH-300 Bruker instrument operating at 75.45 MHz for ¹³C and 300.0 MHz for ¹H spectra. Dioxane

was used as an internal standard. ¹H NMR data were also collected with a Varian EM-390 (90 MHz) spectrometer; routine characterization of organic ligands during synthetic workup procedures were obtained on a Varian EM-360 spectrometer. Infrared spectra were obtained on samples in KBr pellets with a Beckman Acculab-4 instrument and in the Fourier transform mode with an IBM IR/32 FTIR instrument. Differential pulse polarography was carried out on an IBM EC-225 voltammetric analyzer. The standard three-electrode assembly was used. The reference electrode was a NaCl saturated calomel electrode; the working electrode was a glassy-carbon disk. The electrolyte solution was 0.10 M NaCl at 25.0 °C. pH readings were made with an Orion 701 pH meter calibrated with commercial phosphate, biphthalate, and borate buffers. A combination glass/SCE (NaCl) minielectrode was employed.

Ion-Exchange Separations. Anionic complexes of the (CN)₅Fe²⁻ derivatives were isolated by using Bio-Rad AG1-X4 resin in the chloride form. Elutions were made with 0.10, 0.50, 2.00, and 4.00 M NaCl with pH adjustment to control whether the imidazole or imidazolato complexes were to be isolated.

Synthesis of Related Complexes. The 4,5-dicarboxylatoimidazole complex (CN)₅Fe(4,5CO₂imH)⁴⁻ was generated in solution by H₂O₂ oxidation of a 1 × 10⁻⁴ M solution of the Fe(II) complex prepared by stirring the rather insoluble 4,5-dicarboxylic acid with (CN)₅FeOH₂³⁻ for 20 min. Addition of H₂O₂ (3%) solution was followed by filtration of the purple complex solution through glass wool in order to examine the spectral features and kinetic behavior of the (CN)₅Fe(4,5CO₂imH)⁴⁻ and the imidazolato derivative, (CN)₅Fe(4,5CO₂im)⁵⁻. Identical results were obtained with K₂S₂O₈ as the oxidant.

Results and Discussion

Spectra of the Major Species. Spectra of the Fe(III) and Ru(III) complexes of this work confirm or parallel those reported by Johnson, Henderson, and Shepherd² and by Elliott and Shepherd.¹² The characteristic maxima for the various imidazole

(12) Elliott, M. G.; Shepherd, R. E. *Inorg. Chem.* **1987**, *26*, 2067-2073.

(13) Schug, K.; Crean, F. C. *Inorg. Chem.* **1984**, *23*, 853-857.

(14) 2CH₃imH appears to be oxidized on the hours time scale when 0.67 M 2CH₃imH is combined with 0.67 M K₂S₂O₈.

(10) Programs were written by C. R. Johnson and are described in ref 1.

(11) Curtis, N. J.; Brown, R. S. *J. Org. Chem.* **1980**, *45*, 4038-4040.

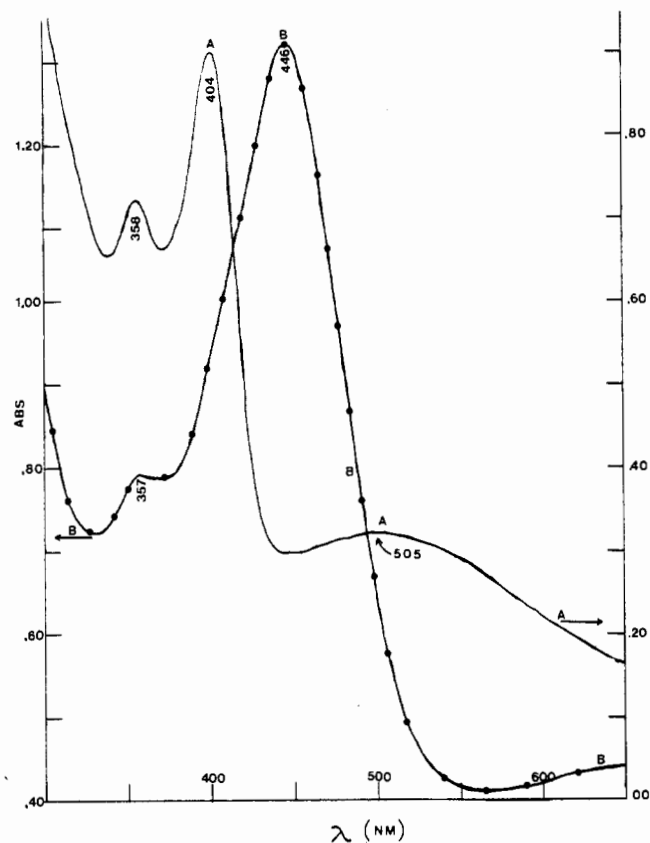


Figure 2. UV-visible spectra of $(\text{CN})_5\text{Fe}^{\text{III}}(2\text{CH}_3\text{imH})^{2-}$ and $(\text{CN})_5\text{Fe}^{\text{III}}(2\text{CH}_3\text{im})^{3-}$ ($[2\text{CH}_3\text{imH}] = 8.43 \times 10^{-3} \text{ M}$): (A) $[(\text{CN})_5\text{Fe}(2\text{CH}_3\text{imH})^{2-}] = 5.62 \times 10^{-4} \text{ M}$; (B) $[(\text{CN})_5\text{Fe}(2\text{CH}_3\text{im})^{3-}] = 5.62 \times 10^{-4} \text{ M}$.

and imidazolato complexes examined in this report are given in Table I. $\text{R} = \text{CH}_3$ substitution causes C-based $d\pi \leftarrow (\pi_1)_L$ LMCT bands of either the imidazole (Figure 2A) or imidazolato (Figure 2B) complexes to be shifted to lower energy relative to that for $\text{R} = \text{H}$, while these bands for the $\text{R} = \text{CO}_2^-$ and CHO complexes are shifted to higher energy (Figures 3, 4, and 8). The $d\pi \leftarrow (\pi_1)_L$ transition becomes a weaker tailing shoulder on the $d\pi \leftarrow (\pi_{2,n})_L$ transition for the $\text{R} = \text{CO}_2^-$ and CHO derivatives; it is fully resolved for the $\text{R} = \text{CH}_3$ complex. This is clearly consistent with the anticipated electron-releasing inductive effect of $\text{R} = \text{CH}_3$ and the withdrawing induction of $\text{R} = \text{CO}_2^-$ and CHO. Smaller energetic influences of the R substituent are observed in the intense LMCT bands in the region of 438 nm for the $(\text{CN})_5\text{Fe}(\text{imR})^{3-}$ complexes, which have been assigned as $d\pi \leftarrow (\pi_{2,n})_L$ transitions.^{2,5b} However, the shifts are in the same order (lower E for $\text{R} = \text{CH}_3$; higher E for $\text{R} = \text{CO}_2^-$ and CHO). The transition energies for the $\text{R} = \text{CHO}$ complexes are higher than for $\text{R} = \text{CO}_2^-$ in concert with its larger σ_p constant. The $d\pi \leftarrow (\pi_1)_L$ transition energies for $(\text{CN})_5\text{Fe}(\text{RimH})^{2-}$ complexes are linear in σ_p (slope $(6.9 \pm 0.4) \times 10^3 \text{ cm}^{-1}/\sigma$; intercept ($\sigma = 0$) $21.2 \times 10^3 \text{ cm}^{-1}$).

Kinetics of the Dissociation of the 2-Methylimidazolato Ligand.

In the previous study of the dissociation of $(\text{CN})_5\text{Fe}(\text{im})^{3-}$, two methods were used to prepare the $(\text{CN})_5\text{Fe}^{\text{III}}(\text{imH})^{2-}$ precursor.¹ These included oxidation of $(\text{CN})_5\text{Fe}(\text{imH})^{3-}$ by H_2O_2 , followed

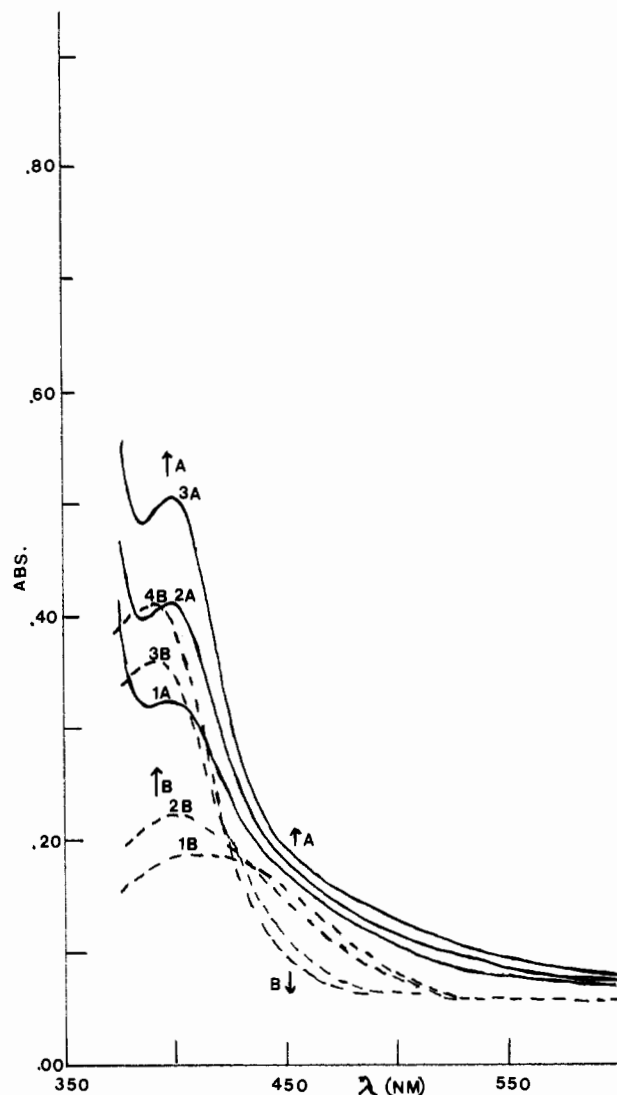


Figure 3. UV-visible spectra of $(\text{CN})_5\text{Fe}^{\text{III}}(2\text{CO}_2\text{imH})^{3-}$ and $(\text{CN})_5\text{Fe}^{\text{III}}(\text{OH})_2^{2-}$ produced by $\text{S}_2\text{O}_8^{2-}$ oxidation: (A) $[(\text{CN})_5\text{Fe}(\text{OH})_2^{3-}]_i = 3.65 \times 10^{-4} \text{ M}$, $[\text{S}_2\text{O}_8^{2-}] = 1.03 \times 10^{-3} \text{ M}$, and $[2\text{CO}_2\text{imH}^-] = 3.72 \times 10^{-2} \text{ M}$ with 1A at 15.0 min, 2A at 30 min, and 3A at 70 min; (B) $[(\text{CN})_5\text{Fe}(\text{OH})_2^{3-}]_i = 3.74 \times 10^{-4} \text{ M}$, $[\text{S}_2\text{O}_8^{2-}] = 1.73 \times 10^{-3} \text{ M}$, and pH 9.20 with 1B at time of mixing, 2B at 12.67 min, 3B at 63.33 min, and 4B at 114 min.

by anion-exchange separation of the desired $(\text{CN})_5\text{Fe}(\text{imH})^{2-}$ product. The alternate procedure used KIO_4 as an excess oxidant to produce $(\text{CN})_5\text{Fe}(\text{imH})^{2-}$ in solution. Neither of these two methods proved to be suitable in the present study to produce the $(\text{CN})_5\text{Fe}(2\text{CH}_3\text{imH})^{2-}$ starting reagent. Neither H_2O_2 or KIO_4 oxidant gave a product of sufficiently low concentration of Fe^{II} complex to prevent catalysis of the Fe^{III} dissociation of $2\text{CH}_3\text{im}^-$ via the Fe^{II} complex.¹ The rate upon addition of the NaOH solution was zero order even in the presence of a large excess of KIO_4 . The H_2O_2 method often produced a product that began loss of $2\text{CH}_3\text{imH}$ before $(\text{CN})_5\text{Fe}(2\text{CH}_3\text{imH})^{2-}$ could be removed from the ion-exchange resin or during storage at 4°C . A stronger oxidant was necessary.

In an effort to suppress the Fe^{II} to a noncatalytic level, $\text{K}_2\text{S}_2\text{O}_8$ was used in a 2-fold molar excess with respect to $(\text{CN})_5\text{Fe}^{\text{III}}(2\text{CH}_3\text{imH})^{3-}$. $(\text{CN})_5\text{Fe}(2\text{CH}_3\text{imH})^{2-}$ produced in the presence of $\text{S}_2\text{O}_8^{2-}$ gave the desired first-order decrease in the absorbance of $(\text{CN})_5\text{Fe}(2\text{CH}_3\text{imH})^{3-}$. The imidazolato species forms by the diffusion-controlled deprotonation of the pyrrole proton upon mixing the $(\text{CN})_5\text{Fe}(2\text{CH}_3\text{imH})^{2-}/\text{S}_2\text{O}_8^{2-}$ solution with NaOH at $\mu = 1.00$. The change in absorbance was followed at 500 nm. Useful data without Fe^{II} catalysis could be obtained only if the $\text{S}_2\text{O}_8^{2-}$ oxidation was allowed to proceed for at least 12 min. At longer contact times the observed absorbance decrease remained

- (15) (a) Zanella, A.; Taube, H. *J. Am. Chem. Soc.* **1971**, *93*, 7166–7173. (b) Pocker, Y.; Meany, J. E.; Nist, B. J. *J. Phys. Chem.* **1967**, *71*, 4509.
 (16) Toma, H. E.; Creutz, C. *Inorg. Chem.* **1977**, *16*, 545–550.
 (17) Henderson, W. W.; Shepherd, R. E.; Abola, J. *Inorg. Chem.* **1986**, *25*, 3157–3163.
 (18) (a) Shepherd, R. E.; Hoq, M. F.; Hoblack, N. *Inorg. Chem.* **1984**, *23*, 3249–3252. (b) Warner, L. W.; Hoq, M. F.; Myser, T. K.; Henderson, W. W.; Shepherd, R. E. *Inorg. Chem.* **1986**, *25*, 1911–1914.
 (19) Shepherd, R. E. *J. Am. Chem. Soc.* **1976**, *98*, 3329–3333.
 (20) Sharpe, A. G. *The Chemistry of Cyano Complexes of Transition Metals*; Academic: London, 1976; p 106.

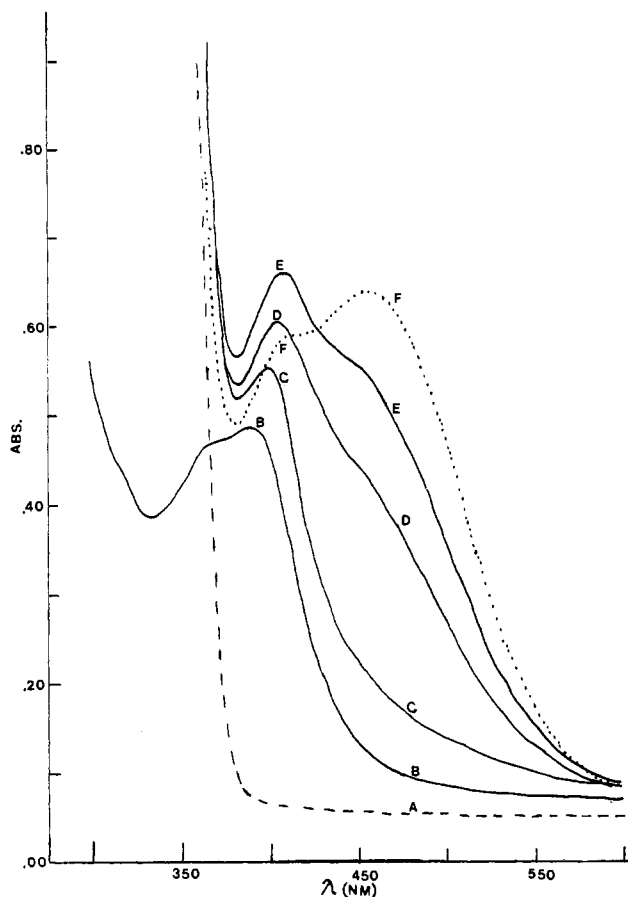


Figure 4. UV-visible spectra of $(\text{CN})_5\text{Fe}^{\text{III}}(2\text{CO}_2\text{imH})^{3-}$ and species 1 produced by H_2O_2 oxidation: (A) 6.52×10^{-2} M $2\text{CO}_2\text{imH}^-$, H_2O_2 blank; (B) $[(\text{CN})_5\text{FeOH}_2^{2-}] = 3.26 \times 10^{-4}$ M, no $2\text{CO}_2\text{imH}^-$, $[\text{H}_2\text{O}_2] = 3.2 \times 10^{-2}$ M, at 90 min, pH 8.09; (C) $[(\text{CN})_5\text{Fe}^{\text{III}}\text{L}^{3-}]_{\text{tot}} = 3.26 \times 10^{-4}$ M, $[2\text{CO}_2\text{imH}^-] = 6.52 \times 10^{-2}$ M, at 90 min, pH 8.85; (D) same as (C) at 220 min; (E) same as (C) at 290 min; (F) same as (C) at 24 h.

Table II. Time Dependence of $\text{S}_2\text{O}_8^{2-}$ Oxidation on the Apparent Dissociation of L^{2-} ^a

time, min	$10^3 k_{\text{obsd}}$	A_{∞}	time, min	$10^3 k_{\text{obsd}}$	A_{∞}
12.5	2.82	0.995	25.0	3.43	0.985
15.0	3.06	0.932	30.0	3.72	0.844
20.0	3.31	0.900	35.0	3.87	0.983

^a Conditions: $[(\text{CN})_5\text{Fe}(2\text{CH}_3\text{imH})^{2-}] = 2.817 \times 10^{-3}$ M; $[(2\text{CH}_3\text{imH})] = 4.225 \times 10^{-2}$ M; 0.500 M NaOH; $\mu = 1.00$; $T = 25.0$ °C.

a first-order process, but the apparent rate constant increased slightly with the total contact time. Data collected with a total oxidation time of 15 ± 3 min are shown in Figure 5 for the dissociation of $(\text{CN})_5\text{Fe}(2\text{CH}_3\text{imH})^{2-}$ at 0.10 and 0.50 M NaOH ($\mu = 1.00$ (NaCl), $T = 25.0$ °C). The dissociation of $(\text{CN})_5\text{Fe}(2\text{CH}_3\text{imH})^{2-}$ is independent of the concentration of excess $2\text{CH}_3\text{imH}$ in the range of $(2.5\text{--}5.7) \times 10^{-2}$ M. The observed first-order rate constants for dissociation of $(\text{CN})_5\text{Fe}(2\text{CH}_3\text{imH})^{2-}$ are determined to be $(1.9 \pm 0.3) \times 10^{-3} \text{ s}^{-1}$ at 0.10 M NaOH and $(2.6 \pm 0.3) \times 10^{-3} \text{ s}^{-1}$ at 0.50 M NaOH.

In order to determine the exact relationship between oxidation time and the observed rate, six kinetic runs under the conditions specified in the procedure were performed at carefully controlled $\text{K}_2\text{S}_2\text{O}_8$ exposure times. The data are given in Table II.

The relatively small variation in A_{∞} supports the idea that the same amount of $(\text{CN})_5\text{Fe}^{\text{III}}\text{OH}^{3-}$ is formed for a given 2-methylimidazole concentration and iron concentration. The data plotted as k_{obsd} vs. time by DIGPLT are linear with a slope of $(7.48 \pm 0.56) \times 10^{-7} \text{ s}^{-2}$ and an intercept of $(2.33 \pm 0.08) \times 10^{-3} \text{ s}^{-1}$. This increase in rate with time would appear to result from the

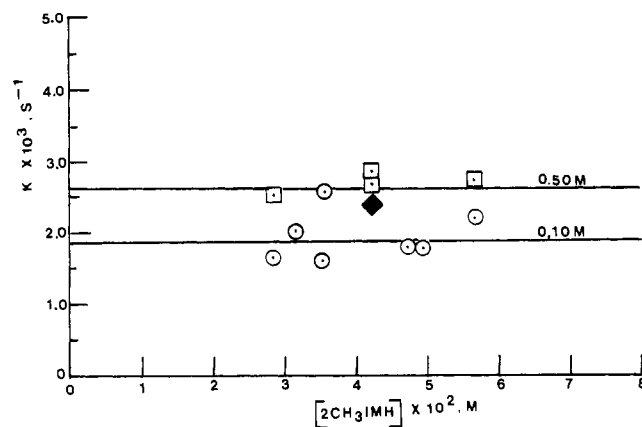


Figure 5. Dissociation of $(\text{CN})_5\text{Fe}(2\text{CH}_3\text{imH})^{2-}$ at 25.0 °C. $[2\text{CH}_3\text{imH}]$ is as given, with $[(\text{CN})_5\text{Fe}(2\text{CH}_3\text{imH})^{2-}]_i = 2.817 \times 10^{-3}$ M, $[\text{OH}^-] = 0.10$ and 0.50 M NaOH, $\mu = 1.00$ (NaCl) and oxidation times of 15 ± 3 min prior to mixing with NaOH.

oxidation of the methyl group to a carboxylate group. At high pH, this will be deprotonated and the resulting negative charge would cause electronic repulsion and a subsequent increase in the dissociation of $2\text{CO}_2\text{im}^{2-}$. It was shown by direct experiments that $2\text{CO}_2\text{imH}^-$ has a much lower affinity for $(\text{CN})_5\text{Fe}^{2+}$. These results are described in a later section. Thus, the intercept value is the unaltered, intrinsic dissociation constant for $2\text{CH}_3\text{im}^-$ at 0.50 M NaOH and $\mu = 1.00$. This experiment appears as the solid diamond point in Figure 5.

The dissociation of $(\text{CN})_5\text{Fe}(\text{im})^{3-}$ was previously observed to have an approach to equilibrium first-order kinetics with $k_{\text{obsd}} = k_d + k_r[\text{imH}]$; k_d was composed of two components, $k_0 + k_1[\text{H}_3\text{O}^+]$.¹ The term in k_0 represents the solvent-assisted dissociation path, $k_1[\text{H}_3\text{O}^+]$ is the proton-assisted dissociation path, and $k_r[\text{imH}]$ represents the contribution from the reverse reaction between $(\text{CN})_5\text{FeOH}^{3-}$ and imH to the changing absorbance. In the present study with $(\text{CN})_5\text{Fe}(2\text{CH}_3\text{imH})^{2-}$, the rate constant is higher at 0.50 M NaOH than at 0.10 M NaOH (both at $\mu = 1.00$ (NaCl) and $T = 25.0$ °C). The higher rate constant at higher $[\text{OH}^-]$ suggests that the k_1 pathway is of little importance in the dissociation of $2\text{CH}_3\text{im}^-$. The higher rate constant at 0.50 M OH^- , compared to that at 0.10 M, is probably an electrolyte effect caused by trading NaCl for NaOH at $\mu = 1.00$. The absence of an appreciable term in $k_r[2\text{CH}_3\text{imH}]$ is also indicated by the data in Figure 5. The steric influence of the 2-methyl group must be responsible for the insensitivity, retarding the reverse rate, $k_r[2\text{CH}_3\text{imH}]$, in the $(\text{CN})_5\text{Fe}(2\text{CH}_3\text{imH})^{2-}$ dissociation.

However, dissociation of $(\text{CN})_5\text{Fe}(2\text{CH}_3\text{imH})^{3-}$ is also an approach to equilibrium kinetic case. This may be seen from the data in Figure 6. The final absorbance of solutions at the same total Fe^{III} concentration varies linearly with the free $[2\text{CH}_3\text{imH}]$ at both 0.10 and 0.50 M NaOH when $[2\text{CH}_3\text{imH}] \gg [\text{Fe}^{\text{III}}]_{\text{tot}}$. More of the $(\text{CN})_5\text{Fe}(2\text{CH}_3\text{imH})^{3-}$ must be present in the final solution as required by equilibrium 6.

Figure 6 reveals large intercept values of 0.58 ± 0.06 and 0.30 ± 0.10 absorbance unit for the 0.10 M OH^- and 0.50 M OH^- data, respectively. This observation implicates the presence of an additional absorbing species with a high extinction coefficient at 500 nm. A candidate for this additional species is $\text{Fe}_2(\text{CN})_{10}^{4-}$, having an ϵ_{500} value of $1.32 \times 10^3 \text{ M}^{-1} \text{ cm}^{-1}$,²¹ compared to ϵ_{500} values of $52 \text{ M}^{-1} \text{ cm}^{-1}$ for $(\text{CN})_5\text{FeOH}^{3-}$ and $1.08 \times 10^3 \text{ M}^{-1} \text{ cm}^{-1}$ for $(\text{CN})_5\text{Fe}(2\text{CH}_3\text{imH})^{3-}$ (this work). The presence of any $\text{Fe}_2(\text{CN})_{10}^{4-}$ dimer is due to the synthetic procedure. It is well-known that $\text{Fe}_2(\text{CN})_{10}^{6-}$ forms competitively with $(\text{CN})_5\text{FeL}^{3-}$, where L is a desired ligand, whenever $[(\text{CN})_5\text{FeOH}_2^{3-}]_{\text{init}} \geq 10^{-4}$ M. The presence of the $\text{Fe}_2(\text{CN})_{10}^{6-}$ species has caused numerous problems

- (21) Espenson, J. H.; Wolenuk, S. G. *Inorg. Chem.* **1972**, *11*, 2034–2041.
- (22) Lister, M. W.; Chlebek, R. W. *Can. J. Chem.* **1966**, *44*, 437–445.
- (23) Kershaw, M. R.; Prue, J. E. *Trans. Faraday Soc.* **1967**, *63*, 1197–1205.
- (24) Basu, M. K.; Das, M. N. *J. Chem. Soc. A* **1968**, 2182–2185.
- (25) Toma, H. E.; Malin, J. M. *Inorg. Chem.* **1973**, *12*, 1039–1045.

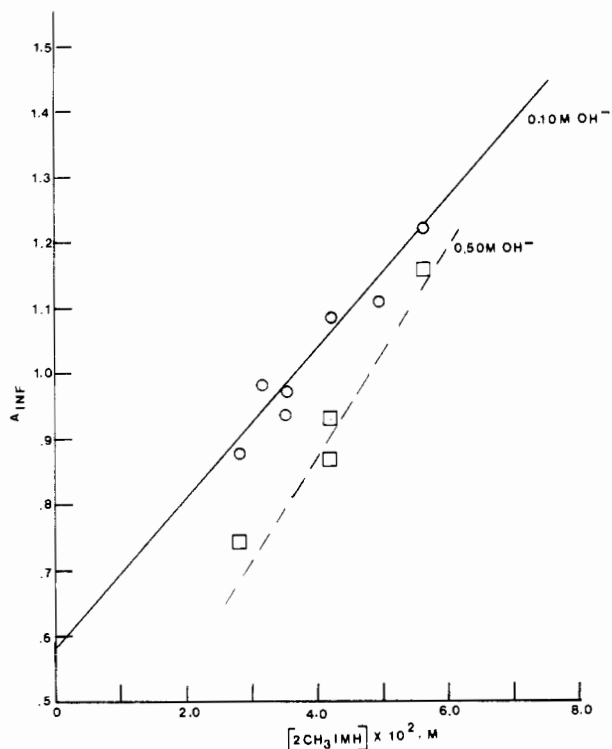


Figure 6. Final equilibrium absorbance for the $(\text{CN})_5\text{Fe}(\text{2CH}_3\text{im})^{3-}$ – $(\text{CN})_5\text{FeOH}^{3-}$ system ($[\text{2CH}_3\text{imH}]$ as given, $[(\text{CN})_5\text{FeL}^{3-}]_{\text{tot}} = 2.817 \times 10^{-3} \text{ M}$, $\mu = 1.00$ (NaCl)): (—) 0.10 M NaOH; (---) 0.50 M NaOH.

in prior kinetic studies of pentacyanoferrate(II) and -(III) complexes.²⁶ In situ oxidation with $\text{S}_2\text{O}_8^{2-}$ of the $(\text{CN})_5\text{Fe}(\text{2CH}_3\text{im})^{3-}$ solution will form both $(\text{CN})_5\text{Fe}(\text{2CH}_3\text{im})^{2-}$ as the major product and $\text{Fe}_2(\text{CN})_{10}^{4-}$ as a minor contaminant. $\text{Fe}_2(\text{CN})_{10}^{4-}$ was prepared separately by the oxidation of $\text{Fe}_2(\text{CN})_{10}^{6-}$ by $\text{S}_2\text{O}_8^{2-}$. Oxidation required several hours for completion at $9.63 \times 10^{-3} \text{ M}$. A spectrum matching the published one for $\text{Fe}_2(\text{CN})_{10}^{4-}$ ²¹ was obtained. Mixing $\text{Fe}_2(\text{CN})_{10}^{4-}$ diluted to $3.85 \times 10^{-4} \text{ M}$ with 0.10 M NaOH revealed a rapid decay of the absorbance band in the region of 535 nm for $\text{Fe}_2(\text{CN})_{10}^{4-}$ with growth of the $(\text{CN})_5\text{FeOH}^{3-}$ spectrum at 385 nm; $t_{1/2} \approx 214 \text{ s}$, and $k \approx 3.2 \times 10^{-3} \text{ s}^{-1}$. Espenson and Wolenuk have reported a two-stage addition of NCS^- and OH^- to $\text{Fe}_2(\text{CN})_{10}^{4-}$; the second addition is much slower with $k \approx 10^{-4} \text{ M}^{-1} \text{ s}^{-1}$.²¹ Assuming a first-order dependence of $[\text{OH}^-]$ on the first reaction with OH^- , a rate constant of $3.2 \times 10^{-2} \text{ M}^{-1} \text{ s}^{-1}$ is implied by our experiments. This compares well with $1.0 \times 10^{-2} \text{ M}^{-1} \text{ s}^{-1}$ for the first addition of NCS^- .²¹ However, these observations rule out $\text{Fe}_2(\text{CN})_{10}^{4-}$ as the additional highly absorbing species at 500 nm that contributes to the intercepts in Figure 6. The two-stage reaction of $\text{Fe}_2(\text{CN})_{10}^{4-}$ with NCS^- ²¹ prompted the investigation of $\text{2CH}_3\text{imH}$ addition to $\text{Fe}_2(\text{CN})_{10}^{4-}$, since excess $\text{2CH}_3\text{imH}$ is also present during the oxidation procedure. The oxidation time is sufficiently long to allow addition of $\text{2CH}_3\text{imH}$ to $\text{Fe}_2(\text{CN})_{10}^{4-}$. Repetitive scanings of the 650–350-nm region, where $\text{Fe}_2(\text{CN})_{10}^{4-}$ exhibits maxima at 535, 395, and 355 nm, were obtained at $[\text{2CH}_3\text{imH}] = 6.33 \times 10^{-2}$ and 0.120 M; $[\text{Fe}_2(\text{CN})_{10}^{4-}]_i = 3.85 \times 10^{-4} \text{ M}$; pH 9.98). A very slight absorbance increase parallel to the $\text{Fe}_2(\text{CN})_{10}^{4-}$ spectrum at all wavelengths above 475 nm was observed with $t_{1/2} \approx 108 \text{ s}$; $k \approx 5.3 \times 10^{-2} \text{ M}^{-1} \text{ s}^{-1}$ for the 0.120 M $\text{2CH}_3\text{imH}$ run. The spectral features of the product solution show maxima at 530, 394, and 354 nm with an ϵ value of $1.45 \times 10^3 \text{ M}^{-1} \text{ cm}^{-1}$ at 500 nm. When this solution was mixed with NaOH to give $[\text{OH}^-] = 0.10 \text{ M}$, the band near 530 nm immediately changed, yielding spectral features at ca. 445 and 650 nm indi-

cative of a cyano–Fe(III)–imidazolato complex.^{1,2} The new species is presumably $\text{Fe}_2(\text{CN})_{10}(\text{2CH}_3\text{im})^{5-}$, analogous to the monocyano-bridged $\text{Fe}_2(\text{CN})_{10}(\text{NCS})^{5-}$ intermediate in the NCS^- addition to $\text{Fe}_2(\text{CN})_{10}^{4-}$. The solution containing $\text{Fe}_2(\text{CN})_{10}(\text{2CH}_3\text{im})^{5-}$ continued to change very slowly with time (Figure 1SM, supplementary material). This suggests the slower monomerization reactions proceed as in the case of NCS^- addition to $\text{Fe}_2(\text{CN})_{10}^{4-}$, but the $\text{Fe}_2(\text{CN})_{10}(\text{2CH}_3\text{im})^{5-}$ species is reasonably stable. The absorbance value at 500 nm remained remarkably constant at 0.39 after the first 16 min through 5.0 h of reaction time. An effective ϵ_{500} value of $8.16 \times 10^2 \text{ M}^{-1} \text{ cm}^{-1}$ was calculated. By contrast, when $(\text{CN})_5\text{Fe}(\text{2CH}_3\text{im})^{2-}$ was generated under conditions of $8.00 \times 10^{-4} \text{ M}$ total Fe(III) and $6.05 \times 10^{-2} \text{ M}$ CH_3imH in order to reduce the presence of $\text{Fe}_2(\text{CN})_{10}^{4-}$ and its $\text{Fe}_2(\text{CN})_{10}(\text{2CH}_3\text{im})^{4-}$ adduct, deprotonation of the coordinated $(\text{CN})_5\text{Fe}(\text{2CH}_3\text{im})^{2-}$ species initiated the equilibration of $(\text{CN})_5\text{Fe}(\text{2CH}_3\text{im})^{3-}$ and $(\text{CN})_5\text{FeOH}^{3-}$ (Figure 2SM, supplementary material). The absorbance is 2-fold less than for $\text{Fe}_2(\text{CN})_{10}(\text{2CH}_3\text{im})^{5-}$ after 1.0 h.

The “infinite time absorbance” that is calculated by the VAINF2 computer-fitting procedure is the sum of absorbances for $(\text{CN})_5\text{Fe}(\text{2CH}_3\text{im})^{3-}$, $(\text{CN})_5\text{FeOH}^{3-}$, and $\text{Fe}_2(\text{CN})_{10}(\text{2CH}_3\text{im})^{5-}$ (A_{dimer}). Assuming a trial equilibrium constant²⁷ of 0.2 for equilibrium 6, $(\text{CN})_5\text{FeOH}^{3-}$ will contribute between 0.080 and 0.100 unit. The glass cell constant is 0.080 unit. Thus, A_{∞} may be set equal to $(A_{(\text{CN})_5\text{Fe}(\text{2CH}_3\text{im})^{3-}} + 0.18 + A_{\text{dimer}})$ over the entire concentration range. The intercept value implies A_{dimer} is about 0.34 at 0.10 M OH^- and 0.12 at 0.50 M NaOH and establishes the maximum $[\text{Fe}_2(\text{CN})_{10}(\text{2CH}_3\text{im})^{5-}] = 4.16 \times 10^{-4} \text{ M}$ at 0.10 M OH^- and $1.47 \times 10^{-4} \text{ M}$ at 0.50 M OH^- . The total analytical concentration of $2.817 \times 10^{-3} \text{ M}$ for $(\text{CN})_5\text{Fe}^{\text{III}}$ species is reduced to an effective value $[\text{Fe}^{\text{III}}]_{\text{tot}}'$, available for equilibrium of the monomeric reactants via eq 6. These values are then $1.99 \times 10^{-3} \text{ M}$ at 0.10 M OH^- and $2.52 \times 10^{-3} \text{ M}$ at 0.50 M for $[\text{Fe}^{\text{III}}]_{\text{tot}}'$.

The relationship between the final absorbance and the equilibrium constant K' for reaction 6 is given by eq 7 when $K' \gg [\text{2CH}_3\text{imH}]$.

$$A_{\infty} = \left(\frac{\epsilon_{\text{FeL}} b}{K'} \right) [\text{Fe}^{\text{III}}]_{\text{tot}}' [\text{2CH}_3\text{imH}] + 0.18 + A_{\text{dimer}} \quad (7)$$

An alternate interpretation for the highly absorbing species is also possible. In this approach a different imidazolato-bridged dimer, $\text{Fe}_2(\text{CN})_{10}(\text{2CH}_3\text{im})^{5-}$, results from the equilibrium between $(\text{CN})_5\text{Fe}(\text{2CH}_3\text{im})^{3-}$ and $(\text{CN})_5\text{FeOH}^{3-}$. An expression with terms parallel to those in eq 7 are obtained.²⁸ The only difference in the derived expression is the meaning of the correction term A_{dimer} . The alternatively derived expression for A_{dimer} shows an inverse dependence on $[\text{OH}^-]$, which is consistent with the lower intercept value at 0.50 M OH^- compared to that for the 0.10 M data in Figure 6. There is the additional difference in meaning of the two different $\text{Fe}_2(\text{CN})_{10}(\text{2CH}_3\text{im})^{5-}$ species. If the imidazolato forms via addition of $\text{2CH}_3\text{imH}$ to $\text{Fe}_2(\text{CN})_{10}^{4-}$ followed by deprotonation, the $\text{Fe}_2(\text{CN})_{10}(\text{2CH}_3\text{im})^{5-}$ complex is cyano-bridged and the species is never at kinetic equilibrium with the dominant species $(\text{CN})_5\text{Fe}(\text{2CH}_3\text{im})^{3-}$ and $(\text{CN})_5\text{FeOH}^{3-}$. If the

(27) The trial value was obtained without correction for the presence of $\text{Fe}_2(\text{CN})_{10}(\text{2CH}_3\text{im})^{5-}$ from eq 7.

(28) Assuming formation of the imidazolato-bridged dimer in a cell with $b = 1.00 \text{ cm}$:

$$(\text{CN})_5\text{Fe}(\text{2CH}_3\text{im})^{3-} + (\text{CN})_5\text{FeOH}^{3-} \xrightleftharpoons{K_D} (\text{CN})_5\text{Fe}(\text{2CH}_3\text{im})\text{Fe}(\text{CN})_5^{5-} + \text{OH}^-$$

$$A_{\infty} = [(\text{CN})_5\text{FeOH}^{3-}] \left(\frac{\epsilon_{(\text{CN})_5\text{Fe}(\text{2CH}_3\text{im})^{3-}} [\text{2CH}_3\text{imH}]}{K'} + \epsilon_{(\text{CN})_5\text{FeOH}^{3-}} \right) + 0.080 + \frac{\epsilon_{\text{dimer}} K_D [\text{2CH}_3\text{imH}] [(\text{CN})_5\text{FeOH}^{3-}]^2}{[\text{OH}^-]}$$

$$A_{\text{dimer}} = \frac{\epsilon_{\text{dimer}} K_D [\text{2CH}_3\text{imH}]}{K' [\text{OH}^-]} [(\text{CN})_5\text{FeOH}^{3-}]^2$$

(26) (a) Emschwiller, G.; Jørgensen, C. K. *Chem. Phys. Lett.* **1970**, *5*, 561. (b) Blesa, M. A.; Funai, I. A.; Morando, P. J.; Olabe, J. A.; Aymonino, P. J.; Ellenrieder, G. *J. Chem. Soc., Dalton Trans.* **1978**, 1610. (c) Davies, G.; Garafalo, A. R. *Inorg. Chem.* **1980**, *19*, 3543.

correct interpretation involves formation of the imidazolato-bridged species (CN)₅Fe(2CH₃im)Fe(CN)₅⁵⁻ from an equilibrium with the monomers, the linear dependence in [2CH₃imH] as shown in Figure 6 implies that [Fe^{III}]_{tot}′ ≈ [(CN)₅FeOH³⁻]. With this approximation, the leading two terms in eq 7 or the alternate expression²⁸ are the same. After the experimental intercepts are corrected for the cell correction and the small absorbance of (CN)₅FeOH³⁻, estimates of ε_{dimer} = 8.2 × 10² M⁻¹ cm⁻¹ and the previously evaluated values of [Fe^{III}]_{tot}′ were used to evaluate an equilibrium constant K_D for formation of (CN)₅Fe(2CH₃im)Fe(CN)₅⁵⁻ from the (CN)₅Fe(2CH₃im)³⁻ and (CN)₅FeOH³⁻ monomers.²⁸ Reasonably consistent values of K_D = 61 and 57 are found at 0.10 and 0.50 M OH⁻, respectively. Since virtually the same amounts of absorbing species are produced whether the starting system is the cyano-bridged Fe₂(CN)₁₀(2CH₃imH)⁴⁻ complex added to 0.10 M OH⁻, 2CH₃imH added to (CN)₅FeOH³⁻, or the OH⁻-induced equilibration of (CN)₅Fe(2CH₃im)³⁻ and (CN)₅FeOH³⁻, it seems most likely that an imidazolato-bridged (CN)₅Fe(2CH₃im)Fe(CN)₅⁵⁻ species is the source of the additional absorbance at 500 nm. Furthermore, the large concentrations of the species causing the intercept absorbance (ca. 4.2 × 10⁻⁴ M at 0.10 M OH⁻, 14.9% of [Fe^{III}]_{tot}′; 1.47 × 10⁻⁴ M at 0.50 M OH⁻, 5.2% of [Fe^{III}]_{tot}′) would not seem to be due to Fe₂(CN)₁₀⁴⁻ considering the care that was taken to avoid Fe₂(CN)₁₀⁶⁻ upon initial mixing of (CN)₅FeNH₃³⁻ under 10–20-fold excess 2CH₃imH.

With *b* = 1.00 cm, ε for (CN)₅Fe(2CH₃im)³⁻ = 1.08 × 10³ M⁻¹ cm⁻¹ at 500 nm, the calculated [Fe^{III}]_{tot}′ values, and the slopes of 11.13 ± 0.14 at 0.10 M OH⁻ and 14.79 ± 2.37 at 0.50 M OH⁻ from Figure 6, the calculated value of *K*′ is 0.193 at 0.10 M OH⁻ and 0.184 at 0.50 M NaOH. *K*′ can also be shown by simultaneous equilibria to be given by eq 8, where *K*_{FeOH}, *K*_{FeLH}, and

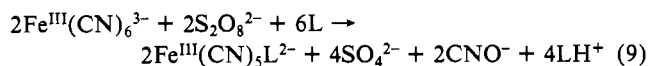
$$K' = \frac{K_w K_{\text{FeOH}}}{K_{\text{a,FeLH}} K_{\text{FeLH}}} \quad (8)$$

*K*_{a,FeLH} represent formation constants of (CN)₅FeOH³⁻ and (CN)₅Fe(2CH₃imH)²⁻ and the acid dissociation constant of (CN)₅Fe(2CH₃imH)²⁻. If the p*K*_a is estimated to be 10.9¹ and *K*_{FeOH} = 4 × 10⁵,²¹ and *K*_w = 1 × 10⁻¹⁴, the value of the association constant for (CN)₅Fe(2CH₃imH)³⁻ is estimated as 1.65 × 10³ M⁻¹ from eq 8 (0.10 M NaOH, 0.90 M NaCl) and 1.73 × 10³ M⁻¹ (0.50 M NaOH, 0.50 M NaCl). The estimate of this formation constant is probably no better than within a factor of 5 due to accumulation of errors in *K*′, *K*_{FeOH}, *K*_a, and *K*_w. However, the value seems reasonable. This compares with 3.4 × 10⁵ for the formation constant of (CN)₅Fe(imH)³⁻; therefore the steric influence of the 2-CH₃ group leads to a complex that is about 206 times less stable. Presence of a 4,5-dimethyl substitution on the imidazole ring reduces the affinity of 4,5-dimethylimidazole by a factor of 193 in the (CN)₅Fe^{II}(4,5CH₃imH)³⁻ complex, where steric influences would be similar.¹⁹

Cyanide vs. 2-Methylimidazole Oxidation by S₂O₈²⁻. In order to determine whether CN⁻ or 2CH₃imH was attacked by K₂S₂O₈ in the (CN)₅Fe(2CH₃imH)²⁻ oxidation, a solution of Fe^{III}(CN)₆³⁻ was made with a large excess of K₂S₂O₈ (0.147 M) and at least a 10-fold molar excess of 2-methylimidazole (0.141 M). The solution was stored in the dark. The solution showed a definite change in its spectrum with a shift toward the UV region as monitored hourly (see Figure 3SM, supplementary material). Precipitate formation occurred after ~3 days. Solutions with lower K₂S₂O₈ concentrations showed similar, but much less dramatic, changes in absorption. No detectable change was observed in solutions stored without K₂S₂O₈ in the presence of 2CH₃imH in the dark.

These results can be explained by the formation of (CN)₅Fe^{II}OH₂³⁻ as cyano groups were labilized during oxidation of Fe^{III}(CN)₆³⁻. Oxidation of coordinated CN⁻ was not recognized in previous studies of the Fe(CN)₆⁴⁻/S₂O₈²⁻ reaction at low and equal concentrations of Fe(CN)₆⁴⁻ and S₂O₈²⁻.^{20,22–24} However, oxidation of CN⁻ in Ru(CN)₆³⁻ by Ce(IV), forming CNO⁻, has been described.¹³ In the Ru(CN)₆³⁻ case, ligand oxidation produces a pool of Ru^{II}(CN)₅OH₂³⁻ in the system. The related

(CN)₅Fe^{II}OH₂³⁻ product could serve the same role here. An overall reaction for this where the (CN)₅FeOH₂³⁻ is scavenged by the excess ligand (L = 2CH₃imH) and the product is oxidized to Fe(III) is



It should be pointed out that the S₂O₈²⁻/Fe(CN)₆³⁻ oxidation of coordinated CN⁻ was studied at approximately 30 times the [S₂O₈²⁻] as present in studies of the dissociation of L from (CN)₅FeL²⁻. The absorbance change for CN⁻ oxidation pathways occurs on the hours time scale as opposed to minutes for the acceleration of the (CN)₅Fe(L⁻)³⁻ aquation. This suggests attack of S₂O₈²⁻ on the 2-methylimidazole only for *coordinated* ligand and not free 2CH₃imH ligand in the (CN)₅Fe(2CH₃imH)²⁻ system. Any route to Fe^{II} via scavenging of organic free radicals would induce zero-order kinetics in the ligand exchange over a long time period. This is not observed. Therefore, only coordinated L suffers attack by S₂O₈²⁻ under the concentrations used in the kinetic runs.¹⁴ Also, the oxidation of coordinated CN⁻ at low levels of S₂O₈²⁻ in the kinetic experiments is too slow to be a direct problem in the kinetic studies of 2CH₃im⁻ dissociation from (CN)₅Fe²⁻.

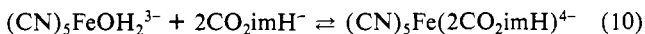
Free-Ligand Spectra. The Li(2CO₂imH) salt exhibits two main transitions in the UV region. Imidazole and 2-methylimidazole show only one π → π* transition at 205 and 195 nm, respectively. Addition of the -CO₂⁻ withdrawing group also extends conjugation with the parent ring. The π → π* transition is red-shifted for 2CO₂imH⁻ to 247 nm. The intensity is comparable to that of the π → π* band of the 2CH₃imH ligand. A much lower intensity band is observed at 330 nm for 2CO₂imH⁻; ε₃₃₀/ε₂₄₇ = 0.035. A third very weak band appears at 290 nm. The π → π* transition is shifted to 244 nm at pH 7.26. At pH ≤ 2, where protonation of both the pyridine N of the imidazole ring and the carboxylate would be anticipated, the π → π* band shifts to 236 nm, and the 330-nm band loses intensity; the original spectrum returns upon raising the pH. These latter facts implicate the 330-nm band with the R = CO₂⁻ moiety; protonation should make any electron release of the R = COOH group much less favorable. The p*K*_a of the imidazole ring N is estimated to be 7.2 on the basis of the percent shift in the π → π* transition of 247 to 242 nm while the 330-nm transition remains essentially unchanged in this pH region. The spectrum is again altered at a pH of 11.5. The transitions are red-shifted to 248 and 336 nm. Formation of the imidazolato form, which is stabilized by the R = CO₂⁻ withdrawing group, is in concert with this observation as the p*K*_a of the parent imidazole pyrrole hydrogen is 14.2.¹ The lowering of the pyrrole p*K*_a by ca. 2 units by the presence of R = CO₂⁻ is reasonable. Reduction of the p*K*_a of the R = CO₂H group to below 2 is in keeping with the adjacent positive charge of the protonated imidazole ring attached to the CO₂H moiety; thus the p*K*_a should fall below that of HCOOH (p*K*_a = 3.32) by ca. 2 units; e.g. p*K*_a ≈ 1.3.

The spectrum of the 2CHOimH ligand in water shows an intense transition at 286 nm (pH 8.20) and a smaller band at 211 nm. If the pH is adjusted below pH 3.08, the 286-nm band decreases substantially and the 211-nm band grows; the shift and intensity pattern is reversible by adding NaOH. A new band appears at 308 nm at pH ≈ 12. These changes are supportive of the pyrrole hydrogen deprotonation with the imidazolato form stabilized by R = CHO through withdrawal for the 308-nm species and the neutral 2CHOimH ligand with a 286-nm π → π* transition. Protonation of the pyridine N position does not alter the π → π* transition appreciably, as it is in conjugation with R = CHO. The major shift of the π → π* transition at low pH, far below the pH required to fully protonate the imidazole ring, is consistent with the known acid-catalyzed hydration of aldehydes to produce a dihydroxy-substituted, saturated carbon (R = CH(OH)₂).¹⁵ The loss of conjugation should make this substituent a much poorer donor by loss of the carbonyl unit; indeed the 211-nm transition energy approaches the value of R = CH₃ as the 2-substituent. ¹H chemical shifts for the R = CHO and R

= CH(OH)₂ forms occur in Me₂SO-*d*₆ at 7.60 and 6.08 ppm, respectively. The hydration was catalyzed by addition of CF₃C=OOH in order to observe the 6.08 ppm resonance.

It was shown that 4.25×10^{-2} M 2CO₂imH⁻ with 4.25×10^{-3} M S₂O₈²⁻ retained its 247- and 330-nm bands unchanged for over 17 h at pH 8.50. Similarly, the 2CHOimH free ligand was not oxidized by S₂O₈²⁻ at pH 7.10, retaining the 286-nm transition unchanged. However, the 330-nm band bleached in 24 h with 80% change in the first 17 h with 3.32×10^{-3} M 2CO₂imH⁻ in the presence of 0.0115 M H₂O₂. The species that is formed by this reaction retains a $\pi \rightarrow \pi^*$ transition at 247 nm at pH 1.93. The ¹H NMR spectrum exhibits a singlet (δ 7.20) in the region of the C-4-H and C-5-H resonances. The acidified sample was concentrated to a solid by evaporation at reduced pressure. No band attributable to R = CO₂⁻, CO₂H, or CHO was present in the infrared region (KBr pellet). The neutral organic molecule was extracted with acetone. Therefore, the product appears to be a new imidazole moiety, derivatized at C(2) with a nonconjugated chromophore. The most likely product would have R = CO₂⁻ replaced by R = OH. Water is known to add across the CO₂⁻ bond via H₃O⁺ catalysis. If H₂O₂ serves this role, HCO₃⁻ becomes a leaving group. The presence of R = OH is supported by the absence of an NMR-active ¹H resonance for the C(2) ring position and the location of the $\pi \rightarrow \pi^*$ transition (247 nm) at long wavelength compared to that for imH or 2CH₃imH. The more stable form should be the tautomer in which the proton of the OH group migrates to the adjacent pyridine N of the imidazole ring; it is anticipated that this form predominates in aqueous solution but that the equilibrium form with R = OH would coordinate to metal centers best through the same pyridine N of the imidazole moiety.

2-Carboxylatoimidazole Complex of (CN)₅Fe²⁺. The cationic Ru(II) and Ru(III) centers (NH₃)₅Ru²⁺ and (NH₃)₅Ru³⁺ form stable complexes with 2CO₂imH⁻ that have been isolated by ion exchange and characterized.¹² Evidence was sought for the related (CN)₅Fe³⁺ and (CN)₅Fe²⁺ complexes of 2CO₂imH⁻. The association constant of imidazole (imH) for the Fe(II) species, (CN)₅Fe²⁺, is 3.4×10^5 M⁻¹.¹ The affinity of imH for the Fe(III) species, (CN)₅Fe³⁺, is similarly high with $K_f = 1.8 \times 10^5$.¹⁶ The equivalency of the C-4 and C-5 hydrogens of the imidazole ring, achieved by a rapid tautomerism of the pyrrole hydrogen, is removed upon coordination. The presence of the coordinated imidazole ring is readily determined for diamagnetic complexes by the changes in the chemical shifts for the imidazole ring protons or the ring carbons by means of ¹H and ¹³C NMR, respectively.^{2,17,19} When (CN)₅FeOH₂³⁻, added as the Na₃[(CN)₅FeN₃H₃]₃H₂O salt, was combined with a 4-fold excess of the Li(2CO₂im) salt in D₂O, there was no evidence for formation of the 2CO₂imH⁻ complex (eq 10) for the diamagnetic Fe(II) com-



plex. This is clearly shown by the coincidence of ¹³C chemical shifts of 2CO₂imH⁻ without added (CN)₅FeOH₂³⁻, as shown in Figure 7. ¹³C chemical shift assignments are noted on the figure.⁹ Equivalent observations were made with ¹H NMR on samples having [2CO₂imH⁻]:[(CN)₅FeOH₂³⁻] up to 10:1. Apparently added anionic charge lowers the affinity of 2CO₂imH⁻ for (CN)₅Fe³⁺.

Although no evidence was found for coordination of 2CO₂imH⁻ with (CN)₅Fe²⁺, the additional π -donor ability favors coordination to Fe(III). A complex of 2CO₂imH⁻ is more likely for (CN)₅Fe²⁺ since it has a smaller negative charge. Two oxidizing agents were employed to generate (CN)₅FeOH₂²⁻ in the range of (3.25–4.46) $\times 10^{-4}$ M with 20-, 94-, and 108-fold excesses of 2CO₂imH⁻. The pH was adjusted to 8.09–9.20. Identical [(CN)₅FeOH₂²⁻], [oxidant], and pH were studied in the absence of added 2CO₂imH⁻. Identical results were obtained on four separate trials. The results with S₂O₈²⁻ as the oxidant are shown in Figure 3. Dashed-line curves with no ligand present show the slow oxidation, which yields a decreasing absorbance change in the 450-nm region and a growth of the 390-nm transition of (CN)₅FeOH₂²⁻. By contrast, with 2CO₂imH⁻ in 102-fold excess the spectra (solid lines) exhibit a

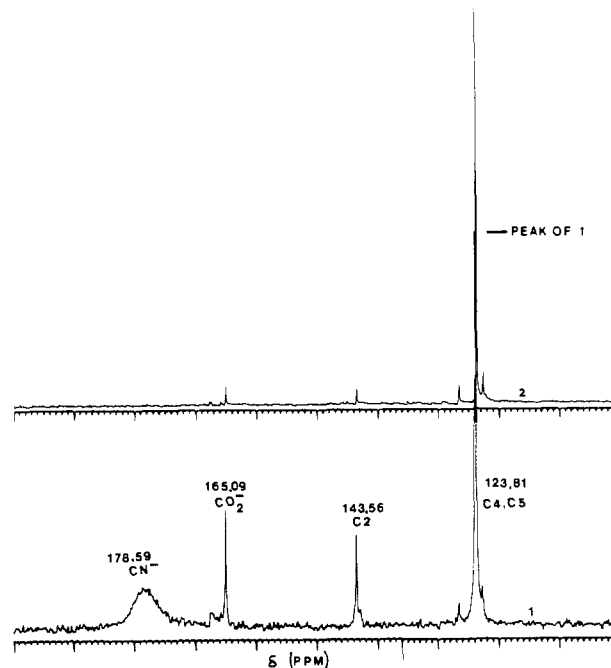
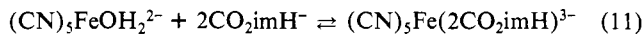


Figure 7. ¹³C NMR spectra of Li(2CO₂imH) in the presence of (CN)₅Fe^{III}(OH₂)₃⁻: (1) 0.80 M Li(2CO₂imH), 0.40 M Na₃[(CN)₅FeN₃H₃]₃H₂O in D₂O, dioxane reference; (2) 0.40 M Li(2CO₂imH) in D₂O, dioxane reference.

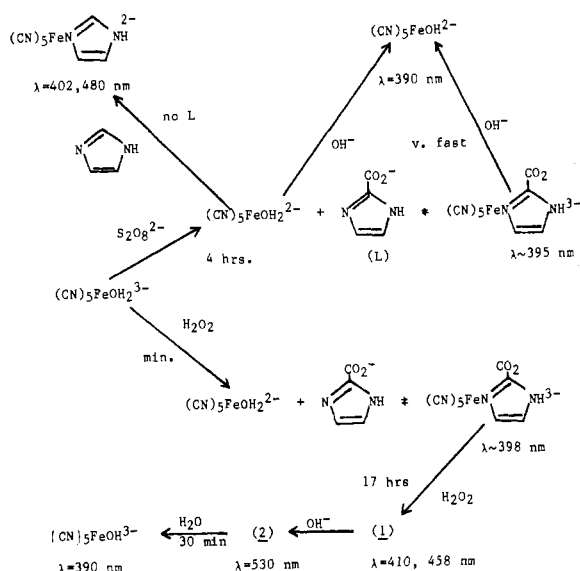
steady increase in absorbance of a weak, tailing band in the 450-nm region and a maximum at 395 nm (pH 8.82). The final spectrum achieved at 5 h remains constant for the next 24 h. When the (CN)₅Fe^{III}(2CO₂imH)₃⁻-containing solution is adjusted to pH ~11, an immediate change to the straw yellow color of (CN)₅FeOH₂³⁻ is observed. No detectable imidazolato intermediate was observed on the conventional spectrophotometric time scale. In the absence of added 2CO₂imH⁻ and in the presence of a 5-fold excess of S₂O₈²⁻, the (CN)₅FeOH₂²⁻ that was produced (dashed curve in Figure 3) was shown to be kinetically labile and quantitatively converted to the imH or 2CH₃imH complexes, when these ligands were added at 0.20 M (530-fold excess). The absence of easily identifiable, characteristic bands for (CN)₅Fe^{III}(2CO₂imH)₃⁻ prompted several studies to show the extent of complexation by 2CO₂imH⁻. (Dimethylamino)pyridine (dmapy) was used as a scavenger for the equilibrium amount of (CN)₅FeOH₂²⁻ in this system (eq 11).^{2,18} These results are



discussed in a subsequent section, but the conclusions are useful. Approximately 27.3% of the total (CN)₅Fe²⁺ is present as the (CN)₅Fe(2CO₂imH)₃⁻ complex, 32.2% is present as (CN)₅FeOH₂²⁻, and 40.5% is present as Fe₂(CN)₁₀⁴⁻ with [2CO₂imH⁻] = 2.40×10^{-2} M (107-fold ligand excess). Therefore, $K_f \approx 35$ M⁻¹ and the affinity of 2CO₂imH⁻ is reduced by 9.7×10^3 relative to that of the parent unsubstituted imidazole ligand. If the steric factor of R = CH₃ is approximately 206 as shown in a prior part of this study and if the overall steric effect for R = CO₂⁻ is assumed to be nearly the same, the anionic charge of 2CO₂imH⁻ vs. imH must account for an additional instability factor of ca. 30. The dissociation of (CN)₅Fe(2CO₂imH)₃⁻ is shown in a later section to be comparable or slower than k_d for (CN)₅Fe(imH)₂²⁻. The substitution of 2CO₂imH⁻ then must also be slower by ca. 30 times, 3 M⁻¹ s⁻¹ compared to 89 M⁻¹ s⁻¹ for imH.¹

Originally H₂O₂ was utilized as the oxidant for (CN)₅FeOH₂³⁻, usually in a 265-fold molar excess. A rapid initial oxidation forms an ion absorbing at 398 nm with 2CO₂imH⁻ present compared to 390 nm with 2CO₂imH⁻ absent (Figure 4). The spectrum at 90 min nearly matches the final one with S₂O₈²⁻ as the oxidant. The spectrum of the (CN)₅FeOH₂³⁻-H₂O₂-2CO₂imH⁻ solution was followed throughout the 24-h period after mixing. A distinct

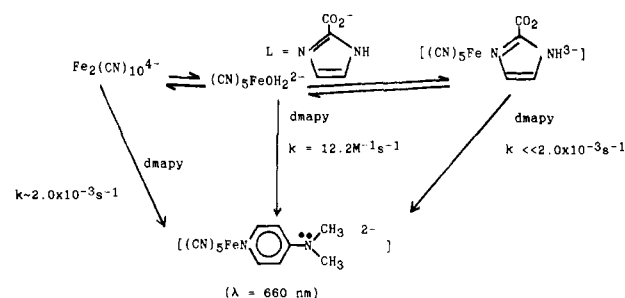
Scheme I



shoulder band appears within 2 h. The 398-nm-absorbing species converts to a new one (1) having a spectrum with maxima at 410 and 458 nm in 17 h; the solution appears orange-yellow. The 458-nm band is modestly more intense. This species (1) is isolated by ion exchange; the ion migrated at [NaCl] > 0.50 M and was eluted readily at 2.0 M. This behavior implicates an ion with a 2- or 3- charge. When the pH of the eluent solution was adjusted to pH ~11, a rose-violet-colored ion (2) is generated having a new spectral maximum at 530 nm. 2 converts to (CN)₅FeOH²⁻ in about 30 min. These spectral changes are shown in Figure 4SM (supplementary material). The sequence of events is shown in Scheme I. The steps interconverting 1, 2, and (CN)₅FeOH²⁻ are the same as the imidazolate dissociation described in eq 1–5. However, the complexes formed in the presence of H₂O₂ and S₂O₈²⁻ at 24 h reaction time are clearly different. The very rapid dissociation of the 395-nm-absorbing complex (via S₂O₈²⁻) compared to the slower dissociation of 2 derived through the 17-h reaction with H₂O₂ suggests that the ligand charge is more negative for the S₂O₈²⁻-derived species. In a separate experiment it was shown that the 2CO₂imH⁻ ligand is not changed by the presence of S₂O₈²⁻ at concentrations identical with those in the complexation studies with (CN)₅Fe²⁺, as determined by no change in the UV ligand bands of the free anion. However, the free ligand anion, 2CO₂imH⁻, is definitely changed by the presence of H₂O₂ within 24 h as described in a prior section. Therefore, one must conclude that the S₂O₈²⁻-derived complex is the authentic (CN)₅Fe^{III}(2CO₂imH)³⁻ complex at equilibrium with (CN)₅FeOH₂²⁻. Ion 1 must be altered in its substituent at the C-2 imidazole ring position from the initial R = CO₂⁻ moiety. Attempts to isolate a purer sample of (CN)₅Fe(2CO₂imH)³⁻, formed via S₂O₈²⁻ oxidation, by means of ion-exchange separation did not succeed because the complexes underwent dissociation and formation of cyanide-bridged dimers on the resin phase prior to elution.

Complexation by dmapy Ligand. It seemed desirable to examine the influence of the presence of 2CO₂imH⁻ on the substitution behavior of (CN)₅FeOH₂²⁻ through equilibrium 11. If complexation with L = 2CO₂imH⁻ occurs as shown in Scheme I, then a rapid substitution of a ligand L that coordinates to (CN)₅FeOH₂²⁻ faster than the reverse dissociation of (CN)₅Fe(2CO₂imH)³⁻ should show at least two separable rate steps: rapid scavenging of the (CN)₅FeOH₂²⁻ followed by a slower reaction that is limited by the dissociation of 2CO₂imH⁻ from (CN)₅Fe(2CO₂imH)³⁻. These studies are shown in Scheme II. Blank studies were carried out on (CN)₅FeOH₂²⁻ produced in a 2-fold excess of S₂O₈²⁻, present to suppress Fe(II) catalysis of the substitution reaction. The reaction was followed at 660 nm, the LMCT maximum of (CN)₅Fe(dmapi)²⁻, in two trials at 117- and

Scheme II



263-fold excesses of dmapi scavenger ligand with [(CN)₅FeOH₂²⁻]_{tot} = (1.89–4.46) × 10⁻⁴ M in 0.050 M borate buffer (pH 9.18; T = 22 °C). A pseudo-first-order reaction, which was over within 150 s, occurs with substitution of the dmapi ligand for 73.2% of the total Fe(III). The second-order rate constant was determined to be 12.2 ± 0.8 M⁻¹ s⁻¹, similar to the imidazole rate constant of 89 M⁻¹ s⁻¹. The latter should have a slight advantage by greater H-bonding to the solvent cage. A much slower second process, which forms (CN)₅Fe(dmapi)²⁻, occurred with a rate of (2.00 ± 0.05) × 10⁻³ s⁻¹ in the absence of 2CO₂imH⁻. It is well-known that (CN)₅FeOH₂²⁻ forms an equilibrium dimer, Fe₂(CN)₁₀⁴⁻, at [Fe(III)] > 10⁻⁴ M.²⁰ The two-step addition of NCS⁻ has been described previously.²¹ Therefore, it is reasonable to assign these steps with dmapi to addition of dmapi to (CN)₅FeOH₂²⁻ (k = 12.2 M⁻¹ s⁻¹) and Fe₂(CN)₁₀⁴⁻ (k = 2.0 × 10⁻³ s⁻¹) in the absence of 2CO₂imH⁻.

Identical samples were obtained by splitting samples of (CN)₅FeOH₂³⁻ prior to the addition of weighed amounts of the K₂S₂O₈ oxidant and Li(2CO₂imH) (or omitting L = 2CO₂imH⁻). It was established that the complexation process involving 2CO₂imH⁻ was complete and equilibrium 11 had been achieved by matching the final spectrum to the studies shown in Figure 3. An aliquot was introduced with rapid mixing of dmapi–borate solution. Significantly less free (CN)₅FeOH₂²⁻ was scavenged in the initial rapid reaction; the amount present as (CN)₅FeOH₂²⁻ was 58.5% of the value determined for the blank study at the same time of equilibration. A second reaction was also observed that matched the rate of addition to Fe₂(CN)₁₀⁴⁻, but the final absorbance value was below the A_∞ value of the blank. After 24 h the A_∞ value with L = 2CO₂imH⁻ present became identical with the value of the blank. Therefore, a third rate process that is at least a power of 10 below that of the Fe₂(CN)₁₀⁴⁻ dissociation is detected. This sets an upper limit of ca. 2.0 × 10⁻⁴ s⁻¹ for this process, which is reasonably close to the dissociation rate of the parent imidazole ligand from (CN)₅Fe(imH)²⁻ (2.6 × 10⁻⁴ s⁻¹).¹ Therefore, we assign the third reaction to the dissociation of (CN)₅Fe(2CO₂imH)³⁻, followed by the [dmapi]-independent scavenging of (CN)₅FeOH₂²⁻, which is slowly produced by this pathway. When the dmapi scavenging study was repeated on 20-h-aged samples with no ligand added and with ligand added, the rate of formation of (CN)₅Fe(dmapi)²⁻ revealed almost complete conversion to Fe₂(CN)₁₀⁴⁻ in the absence of L = 2CO₂imH⁻, but the kinetic behavior of the sample with 2CO₂imH⁻ added was the same at 2 h (initial study) with the 20-h-aged sample. Therefore, the presence of 2CO₂imH⁻ shifts equilibrium 11 to the right and retards Fe₂(CN)₁₀⁴⁻ formation.

2-Imidazolecarboxaldehyde Complexes. When excess 2CHOimH is combined with 4.84 × 10⁻⁴ M (CN)₅FeNH₃³⁻ under Ar, an orange solution forms with a maximum at 454 nm and a slight shoulder at 400 nm in the visible region. The spectrum of (CN)₅Fe(2CHOimH)³⁻ is shown in Figure 8. The ε₄₅₄ value is 1.69 × 10³ M⁻¹ cm⁻¹. The spectrum is reminiscent of the (CN)₅Fe³⁺ complexes with good π-acceptor ligands such as pyrazine. The pyrazine complex has a similar transition at 452 nm, with ε = 5.0 × 10³ M⁻¹ cm⁻¹.²⁵ The Fe(II) complex is reasonably stable toward air oxidation. A 3.70 × 10⁻⁴ M solution of (CN)₅Fe(2CHOimH)³⁻ was prepared and separated from excess 2CHOimH ligand by ion exchange. The ion is readily eluted from AG4-1X resin by 2.0 M NaCl, indicating the 3- ion charge. The

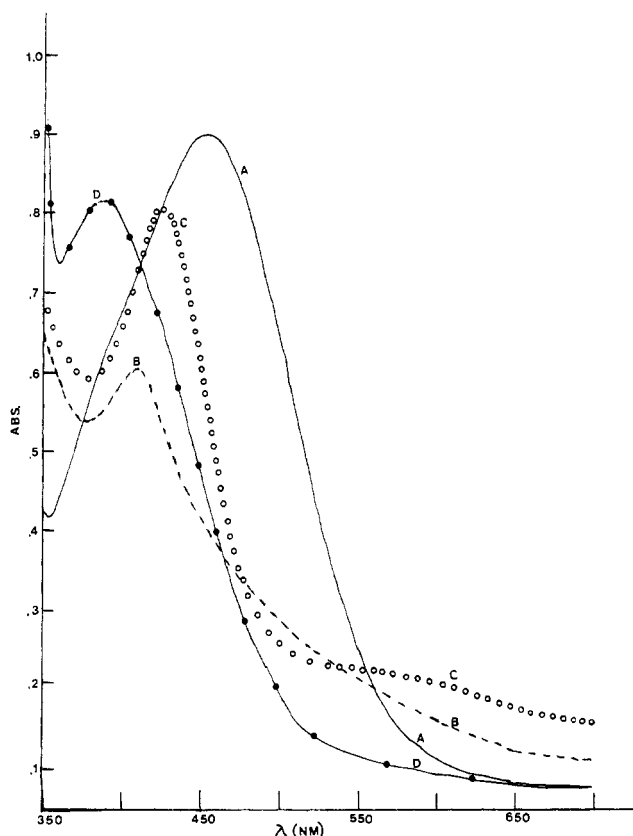


Figure 8. UV-visible spectra of $(\text{CN})_5\text{Fe}^{\text{III}}(\text{2CHOimH})^{3-}$ and $(\text{CN})_5\text{Fe}^{\text{III}}(\text{2CHOimH})^{2-}$: (A) $[(\text{CN})_5\text{Fe}(\text{2CHOimH})^{3-}] = 4.85 \times 10^{-4}$ M, pH 9.02, solution saturated in 2CHOimH, 1.00-cm cell; (B) $[(\text{CN})_5\text{Fe}(\text{2CHOimH})^{2-}] = 4.85 \times 10^{-4}$ M, $[\text{S}_2\text{O}_8^{2-}] = 1.25 \times 10^{-3}$ M, pH 9.02, solution saturated in 2CHOimH; (C) solution (B) adjusted to pH 11. (D) $(\text{CN})_5\text{FeOH}^{3-}$ dissociation product of (C).

spectrum of $(\text{CN})_5\text{Fe}(\text{2CHOimH})^{3-}$ in 2.0 M Na^+ exhibits the MLCT band shifted to 435 nm with the same shoulder at 400 nm at pH 9.24; the ligand $\pi \rightarrow \pi^*$ band appears at 288 nm. High electrolyte concentrations are known to shift LMCT bands of $(\text{CN})_5\text{FeL}^{2-}$ species.¹⁸ At pH 10.17 the two bands are merged with a broadened maximum at 412 nm. Since the free ligand itself is deprotonated at pH ~ 12 , it would appear that the imidazolato form remains coordinated to Fe(II) at pH ≥ 10 . The effect of this change was reversed to the 435-nm initial spectrum with HCl. A loss in the intensity of this band occurs below pH 5.74. At pH 3.64 two peaks in the $\pi \rightarrow \pi^*$ region are found at 288 and 210 nm. Therefore, in the acid region 2CHOimH dissociates from $(\text{CN})_5\text{Fe}(\text{2CHOimH})^{3-}$, as does the parent $(\text{CN})_5\text{Fe}(\text{imH})^{3-}$ system. However, in the case of 2CHOimH, when the ligand dissociates at pH ~ 3.6 the carbonyl group undergoes a rapid hydration to form the imidazolium species with $\text{R} = \text{CH}(\text{OH})_2$.¹²

A differential pulse polarogram ascertained the value of E° for the $(\text{CN})_5\text{Fe}(\text{2CHOimH})^{2-/3-}$ couple to be 0.42 V vs. NHE. Since E° for $(\text{CN})_5\text{Fe}(\text{pz})^{2-/3-}$ is 0.55 V,^{4,16} the electrochemical data imply 2CHOimH is a modestly strong π acceptor toward $(\text{CN})_5\text{Fe}^{3-}$. The comparisons for similar systems are described in detail in ref 4.

In a separate experiment 2CHOimH was shown to be inert to oxidation with $\text{S}_2\text{O}_8^{2-}$ ($[\text{S}_2\text{O}_8^{2-}] = 2.55 \times 10^{-3}$ M). However, when $[\text{S}_2\text{O}_8^{2-}] = 1.25 \times 10^{-3}$ M and $[(\text{CN})_5\text{Fe}(\text{2CHOimH})^{3-}] = 4.00 \times 10^{-4}$ M, the Fe(II) complex was smoothly oxidized in 17 h with the loss of the MLCT band at 454 nm. The product spectrum shows a maximum at 406 nm with a long charge-transfer tail sloping off from 406 to 600 nm. A similar spectrum was obtained in 2.0 min with 4.20×10^{-2} M H_2O_2 . The behavior of this species toward OH^- implicates the product of either the $\text{S}_2\text{O}_8^{2-}$ or H_2O_2 oxidation as being the Fe(III) complex $(\text{CN})_5\text{Fe}(\text{2CHOimH})^{2-}$ (Figure 8). Rapid deprotonation of $(\text{CN})_5\text{Fe}(\text{2CHOimH})^{2-}$ gave a green ion (Figure 8) that exhibited maxima at 428 and 575 nm,

compared to the same transitions at 438 and 625 nm for the parent $(\text{CN})_5\text{Fe}(\text{im})^{3-}$. $(\text{CN})_5\text{Fe}(\text{2CHOimH})^{3-}$, which was prepared by adjustment of the pH to ≥ 12 , underwent a slow, smooth conversion to $(\text{CN})_5\text{FeOH}^{2-}$ through dissociation of the imidazolato form of the ligand. The process for dissociation is markedly accelerated in the solution generated by H_2O_2 oxidation. As before, it would appear that although H_2O_2 is sufficiently strong to cause nearly quantitative oxidation for spectral work, enough Fe(II) is maintained at a steady-state, catalytic level to accelerate the ligand-exchange processes of the major Fe(III) species, $(\text{CN})_5\text{Fe}^{\text{III}}\text{L}$, including the dissociation of the imidazole form of the $\text{R} = \text{CHO}$ derivative. This is the same finding as for the $\text{R} = \text{CH}_3$ case described in detail in a previous section of this text.

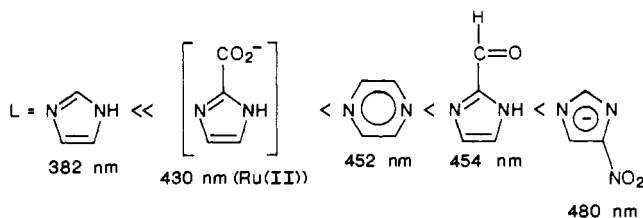
Nature of Species 1 and 2 of Scheme I. H_2O_2 was shown to remove the $\text{R} = \text{CO}_2^-$ group from the free ligand $2\text{CO}_2\text{imH}^-$ (see Free-Ligand Spectra). It is noteworthy that $\text{S}_2\text{O}_8^{2-}$ did not oxidize or change either $2\text{CO}_2\text{imH}^-$ or 2CHOimH on the time scale for ligand substitution and oxidation to the Fe(III) derivatives $(\text{CN})_5\text{Fe}(\text{2CO}_2\text{imH})^{3-}$ and $(\text{CN})_5\text{Fe}(\text{2CHOimH})^{2-}$.

When $2\text{CO}_2\text{imH}^-$ was treated with H_2O_2 and the altered ligand was recovered by extraction, it did not form the same species with $(\text{CN})_5\text{Fe}^{2-}$ as has been identified by the pathway shown in Scheme I yielding **1** (Figure 5SM, supplementary material).

In the presence of H_2O_2 for oxidation of the $(\text{CN})_5\text{FeOH}_2^{3-}$ or $(\text{CN})_5\text{FeL}^{3-}$ complexes, a spectrum appeared in 2 days that had the features for the LMCT transitions of π_1 at ca. 470 nm and $\pi_{2,n}$ at 402 nm, which are very similar to bands of the imidazole complex. When the pH was raised above 11, the dissociation of the imidazolato commenced, yielding $(\text{CN})_5\text{FeOH}^{3-}$. The original spectrum at 15 min reaction time with 2OHimH for this synthetic pathway produced a spectrum with a maximum at 398 nm and showed only a long tailing band out to 550 nm. The initial spectrum was similar to that described for rings having the electronegative or withdrawing groups $\text{R} = \text{CO}_2^-$ or $\text{R} = \text{CHO}$ in the 2-position; however, the spectrum at neither 15 min nor 2 days matched the spectrum of **1**. The dissociation and spectral properties of the imidazolato form ($\lambda_{\text{max}} \cong 435$) do not match those of species **2**. On limited information it appears that the substituent formed during attack of H_2O_2 on the coordinated $(\text{CN})_5\text{Fe}(\text{2CO}_2\text{imH})^{3-}$ complex has a more releasing substituent than $\text{R} = \text{CH}_3$ (as shown in Conclusions) in order to account for the strong 458-nm transition of **1** and the 530-nm band of **2**. The likely candidate would be $\text{R} = \text{CH}_2\text{OH}$, which might accumulate through a Fenton's reagent sequence with Fe complexes and H_2O_2 present, as opposed to only the nucleophilic path for removal of HCO_3^- and insertion of OH when the free ligand and CO_2imH^- react alone. Further work is clearly necessary to sort out the differences in these two routes.

Conclusions. The spectral observations concerning the MLCT and LMCT bands for systems in this study with $\text{R} = \text{CH}_3$, CHO, and CO_2^- present some very interesting results in comparison with those for the parent imidazole complexes, the 4-nitroimidazole cases reported by Eaton and Watkins,⁶ and the numerous prior results with good π -acceptors such as pyrazine.

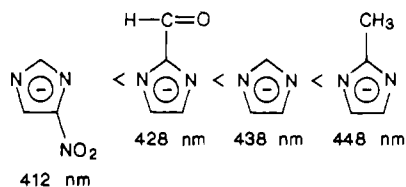
For the Fe(II) series, $(\text{CN})_5\text{Fe}^{\text{II}}\text{L}$, the following MLCT bands are observed:



Since it is known that imidazole, itself, is an extremely poor π -acceptor ligand, the value of the 382-nm transition is an upper limit for this transition energy and probably represents an overlap of the $\text{Fe}^{\text{II}}\text{-CN}$ d-d transition and the related $\text{Fe}^{\text{II}}\text{CN}$ MLCT band. The MLCT transitions of $(\text{CN})_5\text{Fe}^{\text{II}}\text{L}$ species are well-known to shift toward lower energy if electronically withdrawing groups are attached to a pyridine or pyrazine ring, which improves

the π -acceptor power of the ring. However, the pyridine N-heterocycles are legitimately aromatic in character, while the imidazole rings are quasi-aromatic. The results here show that a sufficiently conjugated chromophore induces the same MLCT behavior and increase in the π -acceptor capacity as related chromophores in the pyridine N-heterocycles. The band positions for the cases $R = CO_2^-$, CHO, and NO_2 are in the proper order with respect to their σ_p constants ($\leq 0.13, 0.22, 0.78$).⁷ Electrochemistry of the $(NH_3)_5Ru(2CHOimH)^{2+}$ complex supports $2CHOimH$ as intermediate between pyridine and pyrazine as a π acceptor.¹²

The imidazolato forms of all of the RimH ligands are superior as π donors due to the additional anionic charge density within the five-membered ring. This is borne out by the LMCT $\pi_{2,n}$ band positions of the $(CN)_5Fe^{III}(R-imidazolato)$ series:



The order is inverted as the best π -donor occurs with the best releasing R group, which is $R = CH_3$ in this series. Although the very rapid dissociation of $(CN)_5Fe(2CO_2im)^{4-}$ has prevented the observation of its $\pi_{2,n}$ LMCT band in this study, one would anticipate a value intermediate between those for $R = CHO$ and $R = H$. Therefore, if the $(CN)_5Fe(2CO_2im)^{4-}$ complex were observed in a rapid flow study, for example, the estimated position of the band maximum should be ~ 433 nm.

The steric influence plus the anionic charge of $2CO_2imH^-$ significantly reduces the affinity of this imidazole toward $(CN)_5Fe^{2+}$ by about 5×10^3 in equilibrium constant.^{1,19} This does not appear to be caused by a reduction in the σ donation of the pyridine nitrogen of this ring because the $pK_a \approx 7.2$ is close to the parent imidazole pK_a of 7.0; we note here that the σ -withdrawal influence of $R = CO_2^-$ is compensated by an additional electrostatic attraction for cationic species including H^+ , $Ru(NH_3)_5^{2+}$,

and $Ru(NH_3)_5^{3+,12}$. The cations are not anomalously low in their affinities for $2CO_2imH^-$. In fact the more withdrawing group $R = CHO$ produces stable complexes for both Fe(II) and Fe(III) in the $(CN)_5FeL^{n-}$ series. Therefore, a neutral ligand that will be a slightly poorer σ base than $2CO_2imH^-$ still produces a more stable net interaction with $(CN)_5Fe^{2+}$; the influence is clearly even more important for the Fe(II) system, where $(CN)_5Fe^{3+}$ shows no measurable affinity at all for $2CO_2imH^-$ (cf. ¹³C NMR results, Figure 7).

A number of observations relevant to the ligand substitution processes involving the $Fe(CN)_5^{2-}$ moiety have been observed. The dissociation of the 2-methylimidazolato ligand is reasonably representative and worthy of some detailed consideration.

The current assessment of the dissociation of 2-methylimidazolato ligand from $Fe(CN)_5^{2-}$ is as follows:

(1) The approach to equilibrium rate constant does not have a significant term due to the back-reaction (k_{obsd} appears to be independent of $[L]$), in contrast to the imidazolato case where k_{obsd} increases linearly with $[L]$. This is readily interpreted as a steric inhibition to the rate of substitution of 2-methylimidazole that is absent for the unhindered imidazole.

(2) The presence of the CH_3 group accelerates the k_0 path about 8.9 times at 25.0 °C relative to that for $R = H$, consistent with a steric effect of ca. 1.3 kcal/mol as observed previously.^{1,19} Strained coordination is substantially more prone to redox catalysis for ligand displacement, which causes complications in the study of the $2CH_3imH$ complex.

(3) An oxidation product of $2CH_3imH$, $2CO_2imH^-$, undergoes a similar, but very rapid, ligand dissociation reaction for the imidazolato form of the complex, $(CN)_5Fe(2CO_2im)^{4-}$.

Acknowledgment. We gratefully acknowledge support from NSF Grants CHE 802183 and CHE 8417751.

Registry No. $(CN)_5Fe^{III}(2CH_3imH)^{2-}$, 74354-02-2; $(CN)_5Fe^{III}(2CO_2imH)^{3-}$, 109432-48-6; $(CN)_5Fe^{III}(2CHOimH)^{2-}$, 109432-49-7; $(CN)_5Fe^{II}(2CH_3imH)^{3+}$, 60105-86-4; $(CN)_5Fe^{II}(2CO_2imH)^{4-}$, 109432-50-0; $(CN)_5Fe^{II}(2CHOimH)^{3-}$, 109432-51-1; $S_2O_8^{2-}$, 15092-81-6.

Supplementary Material Available: UV-visible spectra (Figures 1SM-5SM) (5 pages). Ordering information is given on any current masthead page.

Notes

Contribution from the Institute for Physical and Theoretical Chemistry, University of Frankfurt, 6000 Frankfurt am Main, FRG, and Institute for Inorganic Chemistry, University of Witten/Herdecke, 5810 Witten-Annen, FRG

High-Pressure Kinetic Study of an Unusual Hydrolysis Reaction of (Hexafluoroacetylacetonato)bis(ethylenediamine)cobalt(III) in Aqueous Solution

Y. Kitamura¹ and R. van Eldik*

Received February 5, 1987

In general, high-pressure kinetic studies and the associated construction of reaction volume profiles can assist the assignment of the intimate nature of the mechanism for a wide range of thermal and photochemical reactions in solution.²⁻⁴ These include substitution, isomerization, addition/elimination, and electron-transfer processes.

Our interest in recent years in the mechanism of base hydrolysis reactions of Co(III) complexes^{5,6} has led to a series of detailed studies of an unusual, reversible hydrolysis reaction of $Co(en)_2(hfac)^{2+}$ ($en = ethylenediamine$, $hfac = hexafluoroacetylacetonato$) in aqueous solution.^{7,8} During this reaction, addition of OH^- to the carbonyl carbon atom of the $hfac$ ligand occurs, as indicated in reaction 1. The structure of the hydrolysis product was recently confirmed by a crystal structure determination.⁹ A kinetic study⁶

- (1) On leave from the Department of Chemistry, Ehime University, Matsuyama 790, Japan, as a research fellow of the Department of Education of Japan.
- (2) van Eldik, R. *Angew. Chem., Int. Ed. Engl.* **1986**, *25*, 673.
- (3) van Eldik, R. *Comments Inorg. Chem.* **1986**, *5*, 135.
- (4) van Eldik R., Ed. *Inorganic High Pressure Chemistry: Kinetics and Mechanisms*; Elsevier: Amsterdam, 1986.
- (5) Kitamura, Y.; van Eldik, R.; Kelm, H. *Inorg. Chem.* **1984**, *23*, 2038.
- (6) van Eldik, R.; Kitamura, Y.; Piriz Mac-Coll, C. R. *Inorg. Chem.* **1986**, *25*, 4252.
- (7) Aygen, S.; Kitamura, Y.; Kuroda, K.; Kume, R.; Kelm, H.; van Eldik, R. *Inorg. Chem.* **1985**, *24*, 423.
- (8) Kitamura, Y.; van Eldik, R. *Transition Met. Chem.* **1984**, *9*, 257.
- (9) Aygen, S.; Paulus, E. F.; Kitamura, Y.; van Eldik, R. *Inorg. Chem.* **1987**, *26*, 769.

* To whom correspondence should be addressed at the University of Witten/Herdecke.